This includes the cases 2 and 3 as described earlier and other wild-born adults, captive-born adults and adolescents, and colony-born infants, juveniles and adolescents. Among the chimpanzee cases with anti-PGL-I positive serum, there were four with IgG and five with IgM antibodies. Samples from cases 2 and 3 were the only cases that were sera positive for both IgG and IgM anti-PGL-I. On the other hand, among the anti-LAM positive serum samples there were three with IgG and three with IgM antibodies, but only the serum from case 2 was positive for both IgG and IgM antibodies.

A case of leprosy in a chimpanzee in Japan

Haruna is a female chimpanzee who was imported to Japan from West Africa for use in medical research in March 1980 when she was approximately 2 years old [35], and was used for HBV and HCV research. In March 2002, at 21 years she was healthy and was retired to live in a primate sanctuary. In January 2009 at 30 years, her caretaker noticed swelling and nodes on her face. In April, swelling of her eyelids and lips were observed, but no decrease in appetite or other symptoms were observed. Lesions on her face were notable and leontiasis developed. Whole body examination, blood tests, skim smears and biopsies were conducted under anesthesia. The tuberculin reaction was negative, but staining of a nasal swab and a skin smear from a nodule on the left forearm demonstrated acid-fast bacilli. Numerous foamy histiocytes were found in tissue sections of skin biopsies, and diagnosis of lepromatous leprosy was made. PCR analysis for *M. leprae Hsp-70* DNA using skin tissue was positive, but *M. tuberculosis* DNA was not detected. 16S RNA sequencing revealed a 100% match with *M. leprae* genetics. Therefore, it was concluded that the pathogenic bacteria was the same *M. leprae* that causes human leprosy.

On June 1 2009, the MDT for MB regimen was administered as suggested by the WHO by mixing the drug with fruit or juice. After 2 months of MDT, her skin hives disappeared, and after 5 months nasal swab staining for acid-fast bacillus became negative. The treatment was continued for 1 year, as recommended by the WHO [34]. Anti-PGL-I antibody in the preserved sera was negative between 2001 and 2004. In 2008 a false positive was recorded, and the sera turned positive after the onset of symptoms in 2009. After the treatment, the sera again turned negative and it has remained negative for anti-PGL-I antibodies since then. In general, the specificity of anti-PGL-I antibody was uncertain, since the antibody has been detected in some household contacts and even in some healthy individuals in addition to MB patients [15]. However, in Haruna's case, the antibody response against *M. leprae* correlated with acid-fast bacteria detected in her body. Since skin lesions were first noticed in January 2009, the false-positive result of anti-PGL-I in 2008 suggests that *M. leprae* started to grow well before clinical manifestations were evident.

In order to determine the possible origin of the *M. leprae* found in Haruna, SNPs for three reported loci in the *M. leprae* genome were studied [9,10]. PCR amplification followed by direct sequencing identified the SNP type 4 *M. leprae* genotype. This genotype was identified to have originated in West Africa and been introduced to parts of the Caribbean islands and South America (most probably by the slave trade), but has not been found in any other areas. Therefore, infection of Haruna is highly unlikely to have taken place in Japan, particularly given the strict biosafety standards of primate housing facilities in experimental laboratories and the very low prevalence of leprosy in Japan. Evidence strongly suggests that Haruna was infected with *M. leprae* when she was in West Africa by the age of 2 years, and she developed leprosy after an incubation period of at least 30 years [35].

All of the other 13 chimpanzees imported into Japan at the same time lived together in the same cage as Haruna. They have all tested negative for anti-PGL-I antibody. Also, nasal swab staining for acid-fast bacilli and PCR detection of *M. leprae* DNA for 32 other chimpanzees in Japan have all been negative. A survey was conducted at zoos and other facilities which have chimpanzees in Japan, but no other chimpanzees were reported to have had skin symptoms like Haruna. At the sanctuary, no human caretakers have reported skin hives with decreased consciousness [35].

Routes of *M. leprae* infection in chimpanzees

There is a possibility that *M. leprae* might be transmitted among chimpanzees in Africa [30]. Another possibility is that contact with a human patient with *M. leprae* occurred during the 2–3 month period the chimpanzees were housed in outdoor cages while awaiting shipment after capture [27]. In addition, possible transmission from the environment cannot be excluded. There have been some reports of African wild chimpanzees with nasal discharge thought to

be caused by infectious diseases, including leprosy [12]. However, it is difficult to make a diagnosis of leprosy by just observing and without performing a close examination of wild animals. If peripheral neuritis or ulcerations of extremities exist, survival in the wild must be quite difficult.

M. leprae infection is thought to occur when a subject is exposed to a certain number of bacilli either directly or indirectly [12,13]. Although the disease develops after a long incubation period, this progression of disease has never been proven since it is not possible to identify the infection period in human subjects. The life expectancy of chimpanzees is 40–50 years, and the four chimpanzees with leprosy in the present report are considered to be elderly. Although it is not clear what triggered the initiation of active growth of *M. leprae* after the long incubation period, it was speculated in that Haruna's case a recent change in her social group might have resulted in stress that may have transiently impaired her immune system [35].

Conclusion & future perspective

A total of four leprosy cases have been reported in chimpanzees imported from Africa for the purpose of medical experiments. With the most recent case in Japan, the existence of *M. leprae* was proven with DNA analysis. Furthermore, by identification of *M. leprae* SNPs, it was shown that the chimpanzee was infected by the age of 2 years in West Africa, and that the symptoms appeared after an incubation period of at least 30 years. In this case, anti-PGL-I antibody levels were negative before the onset of the disease, turned positive after the onset, and returned again to negative along with the improvement of the symptoms.

These cases also suggest that isolated clinical leprosy in the wild may exist [17,36,37], yet have escaped detection due to reduced fitness and shorter lifespans in the wild. Since the habitat of chimpanzees and other apes is becoming increasingly restricted, contact with humans may become more frequent, increasing the risks of many zoonoses [20,23,36]. Although humans appear to be the major reservoir of *M. leprae* infection, naturally occurring infection has been reported in wild animals, including the nine-banded armadillo and several species of primates [17,19,20,28,29,31–33,35–37]. A recent study found that the same genotypic strain of *M. leprae* was detected at high incidence in wild armadillos and leprosy patients in the southern USA, suggesting that leprosy may be a zoonotic in regions in which armadillos serve as a reservoir [38]. Thus, leprosy is clearly a common disease among humans and other animals. Even after worldwide efforts to reduce the disease burden of leprosy were successfully completed, isolated leprosy cases in wild animals may still exist, which may serve as potential sources of human infection. It will be imperative, therefore, to reconsider the relationship between humans and nonhuman primates in the wild. Careful attention needs to be paid, as both have the possibility to transmit infectious diseases to each other.

Since infection of the four chimpanzees is unlikely to have taken place in the USA or in Japan, they seem to be infected in Africa and disease manifested 5–30 years after infection. However, risk of infection and the clinical manifestations of leprosy depend on multiple factors, but are not restricted to infection during infancy via the nasopharynx. Large numbers of prospective cohort studies of human leprosy patients and their contacts suggest that the risk of leprosy is associated with consanguinity, BCG vaccination and the clinical form of the transmitting cases [39–41]. It was long thought that leprosy might have a strong host genetic component. Genome-wide association studies and searches for susceptibility loci have provided a list of genes associated with host immune response in human leprosylesions [42–45]. Since emergence from dormancy, as well as leprae reaction, appear to be related to stress and changes of immunological status in humans [46], this is possibly also the case with chimpanzees. Research on the role of various stressors in the onset of leprosy and leprae reactions is needed.

Chimpanzees are the closest genetic relatives to humans that have been used for medical research, including infectious diseases research [21–26]. Although chimpanzees and humans have very similar immune systems, fewer genes on the chimpanzee Y chromosome are responsible for immune function [47]. The innate immune systems could also differ, as the living environments of chimpanzees and humans are quite different. Whether these immune system differences affect the occurrence of mycobacterial diseases in chimpanzees is not clear.

The parents of these four chimpanzees must have been killed in order to capture them during their infancy before they were brought to the USA or Japan. Since 1980, approximately 150 chimpanzees have been imported to Japan. They have been used to test the safety of HBV vaccines. During this time, the development of vaccines from human virus carrier plasma was innovative and untested, and the vaccines were

tested on chimpanzees in order to eliminate the possibility of the vaccines containing the active virus. The chimpanzees introduced in this article have contributed not only to the medical experiments for which they were originally intended, but have also unexpectedly contributed to leprosy research. The fourth case discussed in this report, Haruna, fortunately does not have any notable peripheral neuropathy or leprae reactions. She is living her life in the sanctuary peacefully. We truly wish her peace for the rest of her life there.

Financial & competing interests disclosure

This work was supported in part by a grant-in-aid for research on emerging and re-emerging infectious diseases from the Ministry of Health, Labour, and Welfare of Japan for K Suzuki and N Ishii. The authors have no other relevant affiliations or financial involvement with any organization or entity with a financial interest in or financial conflict with the subject matter or materials discussed in the manuscript apart from those disclosed.

No writing assistance was utilized in the production of this manuscript.

Executive summary

Leprosy

- Leprosy is a chronic infectious disorder, caused by *Mycobacterium leprae*, that primarily affects the skin and peripheral nerves.
- Leprosy is suspected to develop after a long period of latency following infection with *M. leprae*, but definitive proof is lacking.
- There is no definitive method that can be used to prove the existence of subclinical infection in humans.

Chimpanzees

- Chimpanzees, as well as great apes including gorillas and orangutans, are members of the Hominoidea superfamily of primates and are humans' closest genetic relatives.
- They are considered the best models for a handful of human diseases, but their status as members of an endangered species and ethical considerations for these highly sentient animals have justifiably limited their use in research.
- They were transported from Africa for the purpose of medical experiments.

Spontaneous leprosy cases in chimpanzees

- Four spontaneous leprosy cases were reported in chimpanzees.
- These chimpanzees have contributed not only to the medical experiments for which they were originally intended, but have also unexpectedly contributed to leprosy research.

Bibliography

Papers of special note have been highlighted as:
- • of interest
- •• of considerable interest

1. Pinheiro RO, de Souza Salles J, Sarno EN, Sampaio EP. *Mycobacterium leprae*-host-cell interactions and genetic determinants in leprosy: an overview. *Future Microbiol.* 6(2), 217–230 (2011).
2. Cole ST, Eiglmeier K, Parkhill J *et al.* Massive gene decay in the leprosy bacillus. *Nature* 409(6823), 1007–1011 (2001).
3. Singh P, Cole ST. *Mycobacterium leprae*: genes, pseudogenes and genetic diversity. *Future Microbiol.* 6(1), 57–71 (2011).
4. Akama T, Suzuki K, Tanigawa K *et al.* Whole-genome tiling array analysis of *Mycobacterium leprae* RNA reveals high expression of pseudogenes and noncoding regions. *J. Bacteriol.* 191(10), 3321–3327 (2009).
5. Akama T, Tanigawa K, Kawashima A, Wu H, Ishii N, Suzuki K. Analysis of *Mycobacterium leprae* gene expression using DNA microarray. *Microb. Pathog.* 49(4), 181–185 (2010).
6. Nakamura K, Akama T, Bang PD *et al.* Detection of RNA expression from pseudogenes and non-coding genomic regions of *Mycobacterium leprae*. *Microb. Pathog.* 47(3), 183–187 (2009).
7. Suzuki K, Nakata N, Bang PD, Ishii N, Makino M. High-level expression of pseudogenes in *Mycobacterium leprae*. *FEMS Microbiol. Lett/* 259(2), 208–214 (2006).
8. Monot M, Honore N, Baliere C *et al.* Are variable-number tandem repeats appropriate for genotyping *Mycobacterium leprae*? *J. Clin. Microbiol.* 46(7), 2291–2297 (2008).
9. Monot M, Honore N, Garnier T *et al.* On the origin of leprosy. *Science* 308(5724), 1040–1042 (2005).
10. Monot M, Honore N, Garnier T *et al.* Comparative genomic and phylogeographic analysis of *Mycobacterium leprae*. *Nat. Genet.* 41(12), 1282–1289 (2009).
11. Job CK, Jayakumar J, Kearney M, Gillis TP. Transmission of leprosy: a study of skin and nasal secretions of household contacts of leprosy patients using PCR. *Am. J. Trop. Med. Hyg.* 78(3), 518–521 (2008).
12. Davey TF, Rees RJ. The nasal discharge in leprosy: clinical and bacteriological aspects. *Lepr. Rev.* 45(2), 121–134 (1974).
13. McDougall AC, Rees RJ, Weddell AG, Kanan MW. The histopathology of lepromatous leprosy in the nose. *J. Pathol.* 115(4), 215–226 (1975).
14. Buhrer-Sekula S. PGL-1 leprosy serology. *Rev. Soc. Bras. Med. Trop.* 41(Suppl. 2) 3–5 (2008).
15. Kampirapap K. Assessment of subclinical leprosy infection through the measurement of PGL-1 antibody levels in residents of a former leprosy colony in Thailand. *Leprosy Rev.* 79(3), 315–319 (2008).
16. Mwanatambwe M, Yajima M, Etuaful S *et al.* Phenolic glycolipid-1 (PGL-1) in Buruli ulcer lesions. First demonstration by immunohistochemistry. *Int. J. Lepr. Other Mycobact. Dis.* 70(3), 201–205 (2002).
17. Meyers WM, Gormus BJ, Walsh GP, Baskin GB, Hubbard GB. Naturally acquired and experimental leprosy in nonhuman primates. *Am. J. Trop. Med. Hyg.* 44(4 Pt 2), 24–27 (1991).
18. Meyers WM, Walsh GP, Brown HL *et al.* Leprosy in a mangabey monkey–naturally

acquired infection. *Int. J. Lepr. Other Mycobact. Dis.* 53(1), 1–14 (1985).

19. Gormus BJ, Wolf RH, Baskin GB *et al.* A second sooty mangabey monkey with naturally acquired leprosy: first reported possible monkey-to-monkey transmission. *Int. J. Lepr. Other Mycobact. Dis.* 56(1), 61–65 (1988).
20. Walsh GP, Meyers WM, Binford CH, Gerone PJ, Wolf RH, Leininger JR. Leprosy – a zoonosis. *Lepr. Rev.* 52(Suppl. 1) 77–83 (1981).
21. Varki A, Altheide TK. Comparing the human and chimpanzee genomes: searching for needles in a haystack. *Genome Res.* 15(12), 1746–1758 (2005).
22. Francis DP, Feorino PM, Broderson JR *et al.* Infection of chimpanzees with lymphadenopathy-associated virus. *Lancet* 2(8414), 1276–1277 (1984).
23. Keele BF, Van Heuverswyn F, Li Y *et al.* Chimpanzee reservoirs of pandemic and nonpandemic HIV-1. *Science* 313(5786), 523–526 (2006).
24. Maynard JE, Berquist KR, Krushak DH, Purcell RH. Experimental infection of chimpanzees with the virus of hepatitis B. *Nature* 237(5357), 514–515 (1972).
25. Tabor E, Gerety RJ, Drucker JA *et al.* Transmission of non-A, non-B hepatitis from man to chimpanzee. *Lancet* 1(8062), 463–466 (1978).
26. Yoshizawa H, Itoh Y, Iwakiri S *et al.* Demonstration of two different types of non-A, non-B hepatitis by reinjection and cross-challenge studies in chimpanzees. *Gastroenterology* 81(1), 107–113 (1981).
27. Donham KJ, Leininger JR. Spontaneous leprosy-like disease in a chimpanzee. *J. Infect. Dis.* 136(1), 132–136 (1977).

▪ **The first leprosy case report in chimpanzees.**

28. Leininger JR, Donham KJ, Rubino MJ. Leprosy in a chimpanzee. Morphology of the skin lesions and characterization of the organism. *Vet. Pathol.* 15(3), 339–346 (1978).
29. Leininger JR, Donham KJ, Meyers WM. Leprosy in a chimpanzee. Postmortem lesions. *Int. J. Lepr. Other Mycobact. Dis.* 48(4), 414–421 (1980).
30. Gormus BJ, Xu KY, Alford PL *et al.* A serologic study of naturally acquired leprosy in chimpanzees. *Int. J. Lepr. Other Mycobact. Dis.* 59(3), 450–457 (1991).

▪ **Results of serological screening of anti-phenolic glycolipid-1 and anti-lipoarabinomannan in chimpanzees in the USA.**

31. Alford PL, Lee DR, Binhazim AA, Hubbard GB, Matherne CM. Naturally acquired leprosy in two wild-born chimpanzees. *Lab. Anim. Sci.* 46(3), 341–346 (1996).
32. Hubbard GB, Lee DR, Eichberg JW, Gormus BJ, Xu K, Meyers WM. Spontaneous leprosy in a chimpanzee (*Pan troglodytes*). *Vet. Pathol.* 28(6), 546–548 (1991).
33. Hubbard GB, Lee DR, Eichberg JW. Diseases and pathology of chimpanzees at the southwest foundation for biomedical research. *Am. J. Primatol.* 24, 273–282 (1991).
34. No authors listed. Chemotherapy of leprosy for control programmes. *World Health Organ. Tech. Rep. Ser.* 675, 1–33 (1982).
35. Suzuki K, Udono T, Fujisawa M, Tanigawa K, Idani G, Ishii N. Infection during infancy and long incubation period of leprosy suggested in a case of a chimpanzee used for medical research. *J. Clin. Microbiol.* 48(9), 3432–3434 (2010).

▪▪ **A case report with extensive genetic analysis of *Mycobacterium leprae*.**

36. Meyers WM, Gormus BJ, Walsh GP. Nonhuman sources of leprosy. *Int. J. Lepr. Other Mycobact. Dis.* 60(3), 477–480 (1992).

▪ **Good review of leprosy in wild animals.**

37. Truman R. Leprosy in wild armadillos. *Lepr. Rev.* 76(3), 198–208 (2005).
38. Truman RW, Singh P, Sharma R *et al.* Probable zoonotic leprosy in the southern United States. *N. Engl. J. Med.* 364(17), 1626–1633 (2011).
39. Fine PE, Sterne JA, Ponnighaus JM *et al.* Household and dwelling contact as risk factors for leprosy in northern Malawi. *Am. J. Epidemiol.* 146(1), 91–102 (1997).
40. Moet FJ, Pahan D, Schuring RP, Oskam L, Richardus JH. Physical distance, genetic relationship, age, and leprosy classification are independent risk factors for leprosy in contacts of patients with leprosy. *J. Infect. Dis.* 193(3), 346–353 (2006).
41. Sales AM, Ponce de Leon A, Duppre NC *et al.* Leprosy among patient contacts: a multilevel study of risk factors. *PLoS Negl. Trop. Dis.* 5(3), e1013 (2011).
42. Bleharski JR, Li H, Meinken C *et al.* Use of genetic profiling in leprosy to discriminate clinical forms of the disease. *Science* 301(5639), 1527–1530 (2003).
43. Mira MT, Alcais A, Nguyen VT *et al.* Susceptibility to leprosy is associated with PARK2 and PACRG. *Nature* 427(6975), 636–640 (2004).
44. Santos AR, Suffys PN, Vanderborght PR *et al.* Role of tumor necrosis factor-α and interleukin-10 promoter gene polymorphisms in leprosy. *J. Infect. Dis.* 186(11), 1687–1691 (2002).
45. Cardoso CC, Pereira AC, de Sales Marques C, Moraes MO. Leprosy susceptibility: genetic variations regulate innate and adaptive immunity, and disease outcome. *Future Microbiol.* 6(5), 533–549 (2011).
46. Mohanty KK, Joshi B, Katoch K, Sengupta U. Leprosy reactions: humoral and cellular immune responses to *M. leprae*, 65kDa, 28kDa, and 18 kDa antigens. *Int. J. Lepr. Other Mycobact. Dis.* 72(2), 149–158 (2004).
47. Kuroki Y, Toyoda A, Noguchi H *et al.* Comparative analysis of chimpanzee and human Y chromosomes unveils complex evolutionary pathway. *Nat. Genet.* 38(2), 158–167 (2006).

JOURNAL OF CLINICAL MICROBIOLOGY, Nov. 2011, p. 3829–3836 Vol. 49, No. 11
0095-1137/11/$12.00 doi:10.1128/JCM.00783-11

Nineteen Cases of Buruli Ulcer Diagnosed in Japan from 1980 to 2010[▽]

Kazue Nakanaga,[1]* Yoshihiko Hoshino,[1] Rie Roselyne Yotsu,[2] Masahiko Makino,[1] and Norihisa Ishii[1]

Leprosy Research Center, National Institute of Infectious Diseases, Tokyo, Japan 189-0002,[1] and Department of Dermatology, National Center for Global Health and Medicine, Tokyo, Japan 162-8655[2]

Received 19 April 2011/Returned for modification 7 June 2011/Accepted 15 August 2011

The etiology, clinical manifestations, and treatment of 19 sporadic cases of Buruli ulcer (BU) in Japan are described. The cases originated in different regions of Honshu Island, with no evidence of patient contact with an aquatic environment. The majority (73.7%) of cases occurred in females, with an average age of 39.1 years for females and 56.8 years for males. All patients developed ulcers on exposed areas of the skin (e.g., face, extremities). Most ulcers were <5 cm in diameter (category I), except in one severe progressive case (category II). Pain was absent in 10 of the 19 cases. Fourteen ulcers were surgically excised, and nine patients needed skin grafting. All cases were treated with various antibiotic regimens, with no reported recurrences as of March 2011. *Mycobacterium ulcerans*-specific IS*2404* was detected in all cases. Ten isolates had identical 16S rRNA gene sequences, which were similar to those of *M. ulcerans*. However, the *rpoB* gene showed a closer resemblance to *Mycobacterium marinum* or *Mycobacterium pseudoshottsii*. PCR identified pMUM001 in all isolates but failed to detect one marker. DNA-DNA hybridization misidentified all isolates as *M. marinum*. The drug susceptibility profile of the isolates also differed from that of *M. ulcerans*. Sequence analysis revealed "*Mycobacterium ulcerans* subsp. *shinshuense*" as the etiologic agent of BU in Japan. Clinical manifestations were comparable to those of *M. ulcerans* but differed as follows: (i) cases were not concentrated in a particular area; (ii) there was no suspected connection to an aquatic environment; (iii) drug susceptibility was different; and (iv) bacteriological features were different.

Buruli ulcer (BU) was first reported in 1935 as a series of unusual painless ulcers in a patient from southeast Australia (2). Thirteen years after the first report, the etiological agent of the ulcer was determined to be *Mycobacterium ulcerans*, a previously unknown mycobacterium (5, 14). During the 1960s, many *M. ulcerans* infections were reported in Uganda, especially in Buruli County, for which this disease was eventually named (3, 32). It is a necrotizing disease of the skin that mostly affects children, producing massive ulcers and permanent, disabling scars. At present, the disease is found primarily in West and Central Africa and in humid tropical areas: BU has been reported in 32 countries, and *M. ulcerans* infection is the third most common mycobacterial infection, after tuberculosis and leprosy. Treatment of progressive cases is difficult and generally requires surgery, usually accompanied by skin grafting and prolonged courses of antibiotics (21, 34).

The first reported case of BU in Japan occurred in 1980 in a 19-year-old woman who had never been abroad (15). The causative agent was isolated and classified as "*Mycobacterium ulcerans* subsp. *shinshuense*" because it was closely related to *M. ulcerans* (31). The disease was not seen again until a 37-year-old woman was affected in 2003 (10). The number of cases increased gradually, until 19 cases had been detected by December 2010 (K. Nakanaga, Y. Hoshino, and N. Ishii, presented at the WHO Annual Meeting on Buruli Ulcer, Geneva, Switzerland, 22 to 24 March 2010). We conducted a comprehensive study using these 19 clinical samples and/or isolated bacteria. Etiology, differential diagnosis, clinical manifestations, and treatments are discussed in this report.

(The preliminary results of this study were presented by K.N. and R. R. Y. in the WHO Annual Meeting on Buruli Ulcer, Geneva, Switzerland, 28 to 30 March 2011.)

MATERIALS AND METHODS

Patients. The research protocol was approved by the institutional review board of the National Institute of Infectious Diseases, Japan. The BU diagnostic criteria were established prior to this study. The primary characteristic was the presence of a clinical lesion, which usually started as a painless subcutaneous nodule, and which secondarily ulcerated with characteristic undermined edges. Other preulcerative forms consisted of papules affecting only the skin, plaques (large, firm, painless, and raised lesions), and edema (a severe form of the disease). Apart from the clinical lesions, at least one of the following criteria must be included for a diagnosis of BU: (i) detection of acid-fast bacilli in a smear from a swab or a biopsy specimen after Ziehl-Neelsen staining, (ii) growth on 7H11 or Ogawa medium, (iii) histopathological confirmation, or (iv) PCR amplification of IS*2404*, an *M. ulcerans*-specific repetitive element. This article is a summary of all BU cases diagnosed to date in Japan. Some have already been published elsewhere as case reports in Japanese and/or English (6, 7, 10, 12, 16, 28, 35).

PCR, sequencing, and phylogenetic analyses. All PCRs targeting IS*2404* (18) were performed on extracted DNA from one or more of the following: fresh skin biopsy specimens, a thin section of formalin-fixed, paraffin-embedded skin, and bacteria isolated from a skin lesion. Briefly, the PCR product, amplified using forward primer PU4F and reverse primer PU7Rbio (Table 1), was electrophoresed on a 2% agarose gel and was stained with ethidium bromide.

The sequences of the internal transcribed spacer between the 16S and 23S rRNA genes (ITS region) and of the 16S rRNA, *rpoB*, and *hsp65* genes were analyzed with the primers listed in Table 1. Amplified PCR products (sizes shown in Table 1) were directly sequenced using the ABI Prism 310 PCR genetic analyzer (Applied Biosystems, Foster City, CA) (16). Sequences were obtained for 1,475- or 1,478-bp (16S rRNA gene), 272-bp (ITS region), 315-bp (*rpoB*), and

* Corresponding author. Mailing address: Department of Mycobacteriology, Leprosy Research Center, National Institute of Infectious Diseases, 4-2-1 Aoba-cho, Higashimurayama-shi, Tokyo 189-0002, Japan. Phone: 81-42-391-8211. Fax: 81-42-394-9092. E-mail: nakanaga@nih.go.jp.

▽ Published ahead of print on 31 August 2011.

TABLE 1. Primer sequences

Primer	Sequence (5′–3′)	PCR target (fragment size [bp])	Reference
PU4F PU7Rbio	GCGCAGATCAACTTCGCGGT GCCCGATTGGTGCTCGGTCA	IS*2404* (154)	18
8F16S 1047R16S	AGAGTTTGATCCTGGCTCAG TGCACACAGGCCACAAGGGA	16S rRNA gene (1,515 or 1,518)	24
830F16S 1542R16S	GTGTGGGTTTCCTTCCTTGG AAGGAGGTGATCCAGCCGCA		
ITSF ITSR	TTGTACACACCGCCCGTC TCTCGATGCCAAGGCATCCACC	16S–23S ITS region (ca. 340)	23
MF MR	CGACCACTTCGGCAACCG TCGATCGGGCACATCCGG	*rpoB* (341)	11
TB11 TB12	ACCAACGATGGTGTGTCCAT CTTGTCGAACCGCATACCCT	*hsp65* (441)	30
RepAF RepAR	CTACGAGCTGGTCAGCAATG ATCGACGCTCGCTACTTCTG	*repA* in pMUM001 (413)	26
ParAF ParAR	GCAAGCTGGGCAATGTTTAT GTCCGGTCCTTGATAGGTCA	*parA* in pMUM001 (501)	26
MUP11F MUP11R	ACCACCCAAGAGTGGAACTG TGTCGTGTCGAGGTATGTGG	Serine/threonine protein kinase in pMUM001 (479)	26
MLSloadF MLSloadR	GGGCAATCGTCCTCACTG CAAGGGCAGTCTTGATTAGG	*mls* load in pMUM001 (560)	26
MLSAT(II)F MLSAT(II)R	AACGTTGAATCCCGTTTTTG GCACCACAAAGGAACGTCTAA	*mlsAT(II)* in pMUM001 (504)	26
TEIIF TEIIR	ATTCAAACGGATGCGAACTG ACATTGCTGGACAAACGACA	Type II thioesterase in pMUM001 (500)	26
MUP045F MUP045R	CAGCAAGTAACGGTGGAACA ACGTGGCCCATTTGTCTTAG	Type III ketosynthase in pMUM001 (496)	26
P450F P450R	CCCACCTCGTCGTTAGTCAT GTGCTCGGTGATCCAGAAGT	P450 in pMUM001 (500)	26

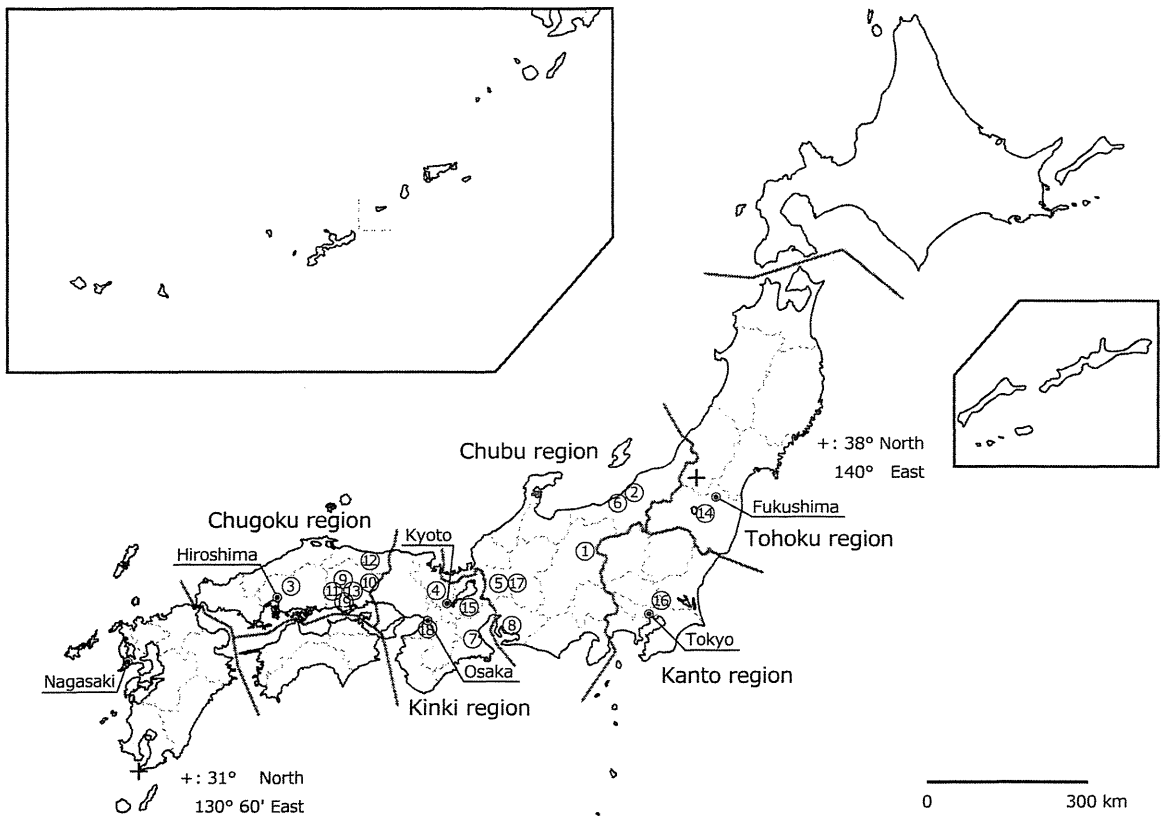

FIG. 1. Distribution of BU patients in Japan. Most of the patients lived in a typical temperate region, and all lived on the island of Honshu. The two plus signs on the map indicate 38°N, 140°E, and 31°N, 130°60′E, placing most of the island in the temperate zone.

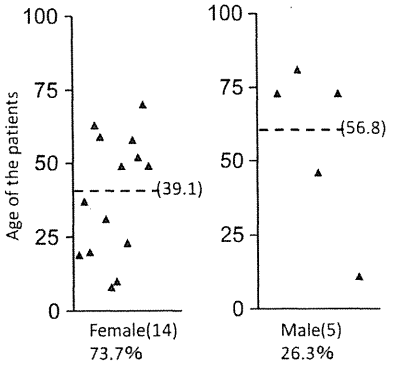

FIG. 2. Ages and genders of BU patients in Japan.

401-bp (*hsp65*) fragments. Ten clinical isolates were compared to six reference strains: *M. ulcerans* ITM 98-912, *M. ulcerans* ATCC 19423^T, *M. ulcerans* Agy99 (25), *Mycobacterium marinum* ATCC 927^T, *M. marinum* clinical isolate LRC 112509, and *Mycobacterium pseudoshottsii* JCM 15466^T. A similarity search was also performed with other mycobacterial reference strains and the 10 clinical strains using the DNA Data Bank of Japan (DDBJ) (8). Phylogenetic analyses were performed using the MEGA software package, version 4.0.2 (build 4028) (29). A tree was constructed using the neighbor-joining method with Kimura's two-parameter distance correction model with 1,000 bootstrap replications.

Finally, primers for eight pMUM001 sequences that encode toxic lipid mycolactone-producing enzymes (26) were used to compare the PCR products of the 10 clinical isolates, *M. ulcerans* ITM 98-912, *M. ulcerans* ATCC 19423^T, *M. ulcerans* Agy99, and *M. pseudoshottsii* JCM 15466^T.

DNA-DNA hybridization assay. A commercially available DNA-DNA hybridization method (DDH Mycobacteria kit; Kyokuto Pharmaceutical Industrial, Tokyo, Japan) was used to identify mycobacterial species isolated from patients (13). The 18 strains in the *Mycobacterium* reference panel included *M. marinum* but not *M. ulcerans*, *M. ulcerans* subsp. *shinshuense*, or *M. pseudoshottsii*.

Growth characteristics and biochemical assay. Culture growth characteristics were determined, and identification was performed, as described previously (16) for 10 of the 11 mycobacterial isolates recovered from patients.

Assay for susceptibility to antimycobacterial drugs. The susceptibilities of the clinical isolates to antibiotics *in vitro* were determined by microdilution (33) using the BrothMIC NTM kit (Kyokuto Pharmaceutical Industrial Co. Ltd., Tokyo, Japan), with modification of the incubation temperature (32°C) and period (2 to 3 weeks). MIC testing was performed in triplicate on different days, with two of three matching MICs used as the criterion for MIC determination.

Nucleotide sequence accession numbers. The DNA sequences of the 16S rRNA (1,475-bp), *hsp65* (401-bp), *rpoB* (315-bp), and ITS (272-bp) fragments from the reference strains (*M. ulcerans* ITM 98-912, *M. ulcerans* ATCC 19423^T, *M. ulcerans* Agy99, *M. marinum* ATCC 927^T, *M. marinum* clinical isolate LRC 112509, and *M. pseudoshottsii* JCM 15466^T) and 10 clinical isolates have been deposited in the International Nucleotide Sequence Database (INSD) through the DDBJ under accession numbers AB548711 to AB548734 and AB624260 to AB624295.

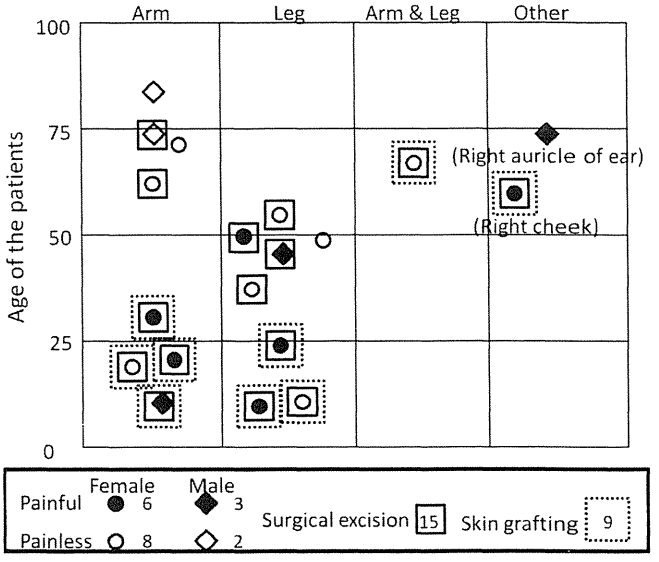

FIG. 4. Localization, pain, and surgical treatment of ulcer lesions by age and gender.

RESULTS

Epidemiology. Nineteen BU cases from Japan have been reported to the WHO BU committee as of December 2010. Many of the *M. ulcerans*-related reports of BU have originated in tropical wetlands. However, Japan is located in eastern Asia, and the majority of the country is covered by mountainous terrain. The 19 cases were distributed between latitudes 34°N and 38°N, in a typical temperate region of Japan.

There was no geographic focal point in the distribution of the BU cases. However, all of the patients lived on Honshu, the largest island of Japan. Seven cases were found in the Chugoku region (western Honshu), 6 in the Chubu region (central Honshu), 4 in the Kinki region (between Chugoku and Chubu), 1 in the Tohoku region (northern Honshu), and 1 in the Kanto region (eastern Honshu) (Fig. 1).

Fourteen (73.7%) subjects were female, and 5 (26.3%) were male. The average age was 39.1 years (range, 8 to 70 years) for the females and 56.8 years (range, 11 to 81 years) for the males (Fig. 2). Despite careful and precise patient interviews, none of the cases could be linked to an aquatic environment.

The affected areas were on exposed sites, such as arms (8

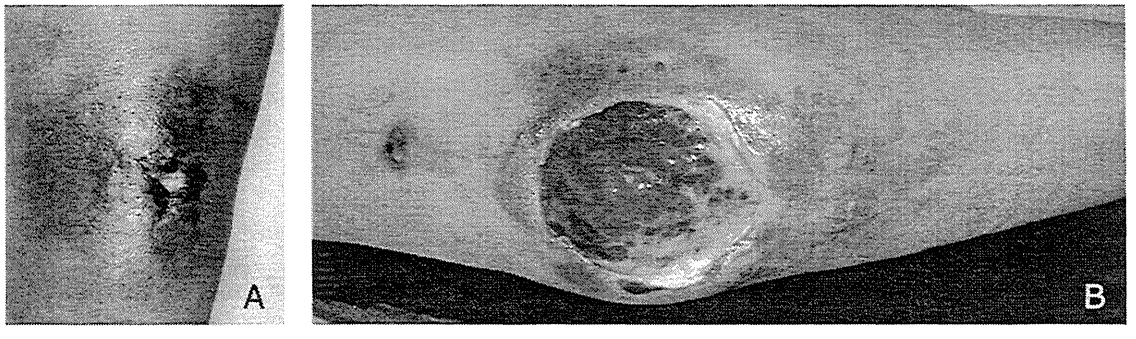

FIG. 3. (A) Buruli ulcer case 8: a category I ulcer on the right forearm. (B) Buruli ulcer case 3: a category II ulcer on the right elbow extensor surface.

TABLE 2. IS*2404* detection in 19 cases of BU in Japan

Case no.	Yr of diagnosis	Origin (region)	Sample type			Isolation period[c]
			Tissue sample[a]	Paraffin section[b]	Isolate	
1	1980	Chubu	NT	NT	P	4 wk
2	2004	Chubu	NT	NT	P	S
3	2006	Chugoku	P	P	P	11 wk
4	2005	Kinki	NT	NT	P	6 wk
5	2007	Chubu	P	P	P	8 wk
6	2007	Chubu	NT	NT	P	S
7	2007	Kinki	NT	NT	P	S
8	2008	Chubu	P	NT	P	11 mo
9	2008	Chugoku	P	NT	NT	NT
10	2009	Chugoku	P	NT	NT	NT
11	2009	Chugoku	P	P	NT	NT
12	2009	Chugoku	P	P	NT	NT
13	2009	Chugoku	NT	P	P	12 wk
14	2009	Tohoku	P	NT	NT	NT
15	2010	Kinki	P	NT	NT	6 wk
16	2010	Kanto	P	P	NT	NT
17	2010	Chubu	P	P	P	5 wk
18	2010	Kinki	P	P	NT	NT
19	2010	Chugoku	P	P	NT	NT

[a] Frozen or fresh skin biopsy sample. NT, not tested; P, positive.
[b] Sliced from a formalin-fixed, paraffin-embedded skin biopsy sample.
[c] S, isolation was successful, but the incubation period was uncertain.

cases), legs (8 cases), the right auricle of the ear (1 case), the right cheek (1 case), and both arms and legs (1 case). While skin ulcer lesions were present in all cases, most were smaller than 5 cm in diameter and were classified as category I (Fig. 3A) (36). In one severe case, the patient presented with a progressive ulcer larger than 10 cm in diameter on the extensor surface of the right elbow, which fell into category II (Fig. 3B). Nine patients (47%) experienced pain, although in many reported cases, BU is painless or only slightly painful (Fig. 4).

Genotypic analysis. PCR screening to detect IS*2404* gave a positive result for at least one of three sample types in all 19 cases. We should note that fresh tissue samples were the source of the template for 13 cases, while formalin-fixed, paraffin-embedded specimens were also used for 9 cases, and all were positive (Table 2). Mycobacteria were successfully isolated in 11 of the 19 cases; however, further bacteriological tests, including genotypic analysis, were performed on 10 available isolates.

The 16S rRNA gene sequences (1,475 bp) of these isolates were identical to each other but partially different from those of *M. ulcerans*, *M. marinum*, and *M. pseudoshottsii* (Table 3). The *hsp65* (401-bp), *rpoB* (315-bp), and internal transcribed spacer (ITS) (272-bp) sequences were also identical among isolates. Sequence analysis identified *M. ulcerans* subsp. *shinshuense* as the bacterium in the clinical samples. Phylogenetic trees based on 16S rRNA and *hsp65* gene sequences showed a close relationship between *M. ulcerans* subsp. *shinshuense* and *M. ulcerans* (Fig. 5A and B). A phylogenetic analysis of the 16S–23S intergenic spacer region showed no differences between *M. ulcerans* subsp. *shinshuense*, *M. marinum*, and *M. ulcerans* and found that *M. pseudoshottsii* is a close relative (Fig. 5C). In contrast, the tree based on the *rpoB* gene showed a closer relationship of *M. ulcerans* subsp. *shinshuense* to *M. marinum* and *M. pseudoshottsii* than to *M. ulcerans*, supporting the premise that *M. ulcerans* subsp. *shinshuense* is distinct from *M. ulcerans* (Fig. 5D).

Next, amplification of eight pMUM001-associated genes was used to determine whether these isolates had genes that encode toxic lipid mycolactone-producing enzymes. All isolates

TABLE 3. Comparison of 16S rRNA gene sequences of 10 *M. ulcerans* subsp. *shinshuense* isolates and related mycobacterial strains

Strain	Country	Nucleotide(s) at the following *Escherichia coli* 16S rRNA gene sequence position(s):								
		95	487–488	492	969	1007	1215	1247	1288	1449–1451[a]
M. ulcerans subsp. *shinshuense*										
ATCC 33728	Japan	T	GG	G	A	G	T	G	G	ACCC---TTTG
JATA753	Japan	T	GG	G	A	G	T	G	G	ACCC---TTTG
0401	Japan	T	GG	G	A	G	T	G	G	ACCC---TTTG
0501	Japan	T	GG	G	A	G	T	G	G	ACCC---TTTG
0701	Japan	T	GG	G	A	G	T	G	G	ACCC---TTTG
0702	Japan	T	GG	G	A	G	T	G	G	ACCC---TTTG
0703	Japan	T	GG	G	A	G	T	G	G	ACCC---TTTG
0801	Japan	T	GG	G	A	G	T	G	G	ACCC---TTTG
0901	Japan	T	GG	G	A	G	T	G	G	ACCC---TTTG
1001	Japan	T	GG	G	A	G	T	G	G	ACCC---TTTG
M. ulcerans										
ITM 98-912	China	T	GG	G	A	G	T	G	G	ACCC---TTTG
ATCC 19423^T	Australia	T	GG	A	A	G	T	G	C	ACCC---TTTG
Agy99	Ghana	T	GG	A	A	G	T	G	C	ACCCTTTTTTG
M. marinum										
ATCC 927^T	United States	T	GG	A	A	G	T	A	A	ACCC---TTTG
112509	Japan	T	GG	A	A	G	T	A	A	ACCC---TTTG
M. pseudoshottsii JCM 15466^T	United States	C	GA	A	G	T	C	A	A	ACCC---TTTG

[a] Hyphens indicate gaps.

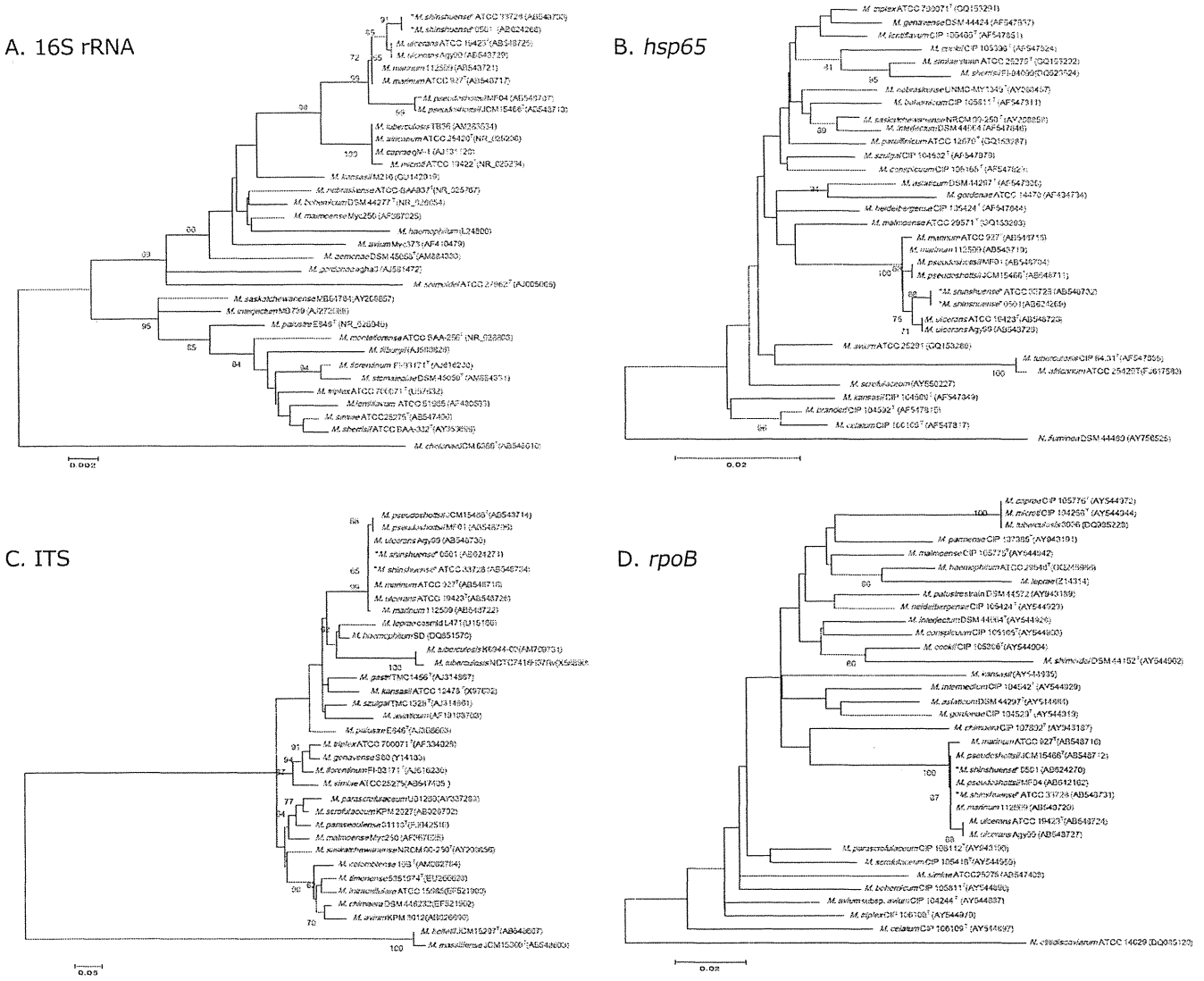

FIG. 5. Phylogenetic analyses of *M. ulcerans* subsp. *shinshuense* based on the 16S rRNA gene (A), the *hsp65* gene (B), the 16S–23S intergenic spacer region (C), and the *rpoB* gene (D).

showed positive results, but as previously reported, the band representing the serine/threonine protein kinase (STPK) gene was absent in *M. ulcerans* subsp. *shinshuense* strains (16). However, this phenomenon was also observed with one strain of *M. ulcerans*, ITM 98-912, that was isolated in China (4). All eight bands were detected in the *M. ulcerans* strains isolated from Australia and Ghana. *M. pseudoshottsii* lacked the band representing P450, but the other seven bands were successfully amplified (Table 4).

A commercially available DNA-DNA hybridization assay was used to verify species identity. The kit contained a reference panel of 18 mycobacterial strains that included *M. marinum* but not *M. ulcerans*, *M. ulcerans* subsp. *shinshuense*, or *M. pseudoshottsii*. All 10 isolates showed clear positive signals for *M. marinum* (Table 5, rightmost column).

Biochemical characteristics. The 10 isolates exhibited the same characteristics: rough colonies and yellow pigmentation, even when grown in the dark. The slowly growing mycobacterium formed visible colonies at 25°C and 32°C on a 2% Ogawa egg slant, but not at 37°C or 42°C. No growth was seen on a medium supplemented with 500 μg/ml *p*-nitrobenzoic acid or 5% NaCl. The isolates were negative for niacin, nitrate reduction, arylsulfatase (3 days), Tween 80 hydrolysis, pyrazinamidase, and iron uptake but were positive for semiquantitative catalase and 68°C catalase and urease. Comparisons between *M. ulcerans* subsp. *shinshuense*, *M. ulcerans*, and *M. marinum* are summarized in Table 5. These results were in accordance with those of a previous report (22) except for the positive result of *M. ulcerans* subsp. *shinshuense* on the urease test.

Drug susceptibility assays. Table 6 shows the results of testing of the susceptibilities of *M. ulcerans* subsp. *shinshuense* ATCC 33728 and *M. ulcerans* subsp. *shinshuense* clinical isolate 0501 to antimicrobial agents. These isolates exhibited high susceptibilities to streptomycin, kanamycin, levofloxacin, and clarithromycin. Notably, *M. ulcerans* subsp. *shinshuense* was more susceptible to streptomycin, kanamycin, and clarithromy-

TABLE 4. PCR detection of eight pMUM001-associated genes in 10 *M. ulcerans* subsp. *shinshuense* isolates and related mycobacterial strains

Strain	Country	Presence or absence of the following pMUM001 marker gene[a]:							
		repA	*parA*	STPK	*mls* (load)	*mlsAT(II)*	TEII	KSIII	P450
M. ulcerans subsp. *shinshuense*									
ATCC 33728	Japan	+	+	−	+	+	+	+	+
JATA753	Japan	+	+	−	+	+	+	+	+
0401	Japan	+	+	−	+	+	+	+	+
0501	Japan	+	+	−	+	+	+	+	+
0701	Japan	+	+	−	+	+	+	+	+
0702	Japan	+	+	−	+	+	+	+	+
0703	Japan	+	+	−	+	+	+	+	+
0801	Japan	+	+	−	+	+	+	+	+
0901	Japan	+	+	−	+	+	+	+	+
1001	Japan	+	+	−	+	+	+	+	+
M. ulcerans									
ITM 98-912	China	+	+	−	+	+	+	+	+
ATCC 19423^T	Australia	+	+	+	+	+	+	+	+
Agy99	Ghana	+	+	+	+	+	+	+	+
M. pseudoshottsii JCM 15466^T	United States	+	+	+	+	+	+	+	−

[a] +, present; −, absent. STPK, serine/threonine protein kinase; TEII, type II thioesterase; KSIII, type III ketosynthase.

cin than the *M. ulcerans* reference strains. Like the *M. ulcerans* reference strains, *M. ulcerans* subsp. *shinshuense* was susceptible to amikacin but resistant to ethambutol, isoniazid, and ethionamide.

Treatment. The 19 patients were treated with various antibiotic regimens. Clarithromycin was effective for many of the Japanese patients (12 cases). Rifampin was successful in the first case and was used thereafter in 9 cases. Attempts at treatment with other medications, alone and in combinations, were also made (Table 7). In 2 cases, the initial choice of antibiotics was ineffective, and they were changed. In 2 other cases, the antibiotic treatment was discontinued due to adverse effects. In addition to antibiotic treatment, 13 patients underwent surgical excision, and 9 needed skin grafting (Fig. 4). No relapses had been reported as of March 2011.

DISCUSSION

This is the first report that comprehensively analyzes both the genotypic and the biochemical profiles of a causative agent of Buruli ulcer in Japan. It is noteworthy that BU in Japan was induced by *Mycobacterium ulcerans* subsp. *shinshuense*, not by *M. ulcerans*. We compared certain characteristics of *M. ulcerans* and *M. ulcerans* subsp. *shinshuense* by several analyses. They are relatively similar; detection of IS*2404* by PCR was the most important test for early diagnosis and differential diag-

TABLE 5. Bacteriological characteristics of 10 *M. ulcerans* subsp. *shinshuense* isolates and closely related mycobacterial strains

Strain	Country	Biochemical characteristic							Identification of *M. marinum*[b]
		Growth rate	Colony morphology	Pigment in dark	Urease activity	Tween 80 hydrolysis	PZase[a] activity	MPB64 production	
M. ulcerans subsp. *shinshuense*									
ATCC 33728	Japan	Low	Rough	Yellow	+	−	−	−	+
JATA753	Japan	Low	Rough	Yellow	+	−	−	−	+
0401	Japan	Low	Rough	Yellow	+	−	−	−	+
0501	Japan	Low	Rough	Yellow	+	−	−	−	+
0701	Japan	Low	Rough	Yellow	+	−	−	−	+
0702	Japan	Low	Rough	Yellow	+	−	−	−	+
0703	Japan	Low	Rough	Yellow	+	−	−	−	+
0801	Japan	Low	Rough	Yellow	+	−	−	−	+
0901	Japan	Low	Rough	Yellow	+	−	−	−	+
1001	Japan	Low	Rough	Yellow	+	−	−	−	+
M. ulcerans									
ITM 98-912	China	Low	Rough	Yellow	+	−	−	−	+
ATCC 19423^T	Australia	Low	Rough	None	−	−	−	−	+
Agy99	Ghana	Low	Rough	Yellow	−	−	−	−	+
M. marinum ATCC 927^T	United States	Medium	Smooth	None	+	+	+	−	+

[a] PZase, pyrazinamidase.
[b] By use of the DDH Mycobacteria kit (Kyokuto Pharmaceutical Industrial, Tokyo, Japan).

TABLE 6. Drug susceptibility test results

Antimycobacterial drug[a]	MIC (μg/ml) for:			
	M. ulcerans subsp. *shinshuense*		*M. ulcerans*	
	ATCC 33728	0501	ATCC 19423^T	Agy99
SM	0.125	0.25	1	4
EB	16	8	16	128
KM	0.25	0.25	1	1
INH	8	8	>32	>32
RFP	0.06	0.06	0.06	0.06
LVFX	0.25	0.5	0.5	8
CAM	0.03	0.06	0.25	0.125
TH	16	8	16	16
AMK	0.5	0.5	0.5	0.5

[a] SM, streptomycin; EB, ethambutol; KM, kanamycin; INH, isoniazid; RFP, rifampin; LVFX, levofloxacin; CAM, clarithromycin; TH, ethionamide; AMK, amikacin.

TABLE 7. Antibiotic treatment regimens for BU cases

Regimen[a]	No. of cases
Single drug	
CAM	2
MINO	1
RFP	1
Two drugs	
CAM, RFP	2
ITZ, MINO	1
LVFX, MINO	1
Three drugs	
CAM, LVFX, RFP	3
CAM, CFPN-PI, NFLX	1
CFPN-PI, LVFX, MINO	1
CAM, MINO, NFLX	1
GRNX, LVFX, MINO	1
Four drugs (EB, LVFX, RFP, SM)	1
Six drugs	
AZM, CAM, CPFX, LVFX, MINO, RFP	1
CAM, EB, GFLX, INH, RFP, SM	1
CAM, CPFX, LVFX, MINO, PZFX, RFP	1

[a] AZM, azithromycin; CAM, clarithromycin; CFPN-PI, cefcapene-pivoxil; CPFX, ciprofloxacin; EB, ethambutol; GFLX, gatifloxacin; GRNX, garenoxacin; INH, isoniazid; ITZ, itraconazole; LVFX, levofloxacin; MINO, minocycline; NFLX, norfloxacin; RFP, rifampin; SM, streptomycin; PZFX, pazufloxacin.

nosis for distinguishing both *M. ulcerans* subsp. *shinshuense* and *M. ulcerans* infections from *M. marinum* infection. Although the DDH Mycobacteria kit could not distinguish *M. ulcerans* and *M. ulcerans* subsp. *shinshuense* from *M. marinum* (Table 5), simultaneous detection of IS*2404* would prevent misidentification. IS*2404* was well amplified from clinical samples and/or isolates in all 19 cases (Table 2). The 16S rRNA gene sequences of *M. ulcerans* subsp. *shinshuense* and *M. ulcerans* are similar, but conserved sites that were different in *M. ulcerans* subsp. *shinshuense* versus *M. ulcerans* were seen (Table 3); these matched perfectly with the sequences reported by Portaels et al. (20) and subsequently found to be useful in discrimination (6, 16). PCR targeting of pMUM001 revealed that all *M. ulcerans* subsp. *shinshuense* isolates lack the band representing the STPK gene, suggesting a small but conservative mutation(s) in *M. ulcerans* subsp. *shinshuense* versus *M. ulcerans* sequences. This PCR test was also applied for detection of a virulent plasmid and for differential diagnosis of *M. ulcerans* versus *M. ulcerans* subsp. *shinshuense* (16). The DNA sequence of the ITS region and the 16S rRNA and *hsp65* genes showed similarity between the *M. ulcerans* subsp. *shinshuense* isolates and *M. ulcerans*. However, the *rpoB* gene showed more similarity to *M. marinum* and *M. pseudoshottsii* than to *M. ulcerans* (Fig. 5). These data were suggestive of the evolutionary paths of these related mycobacterial species (9).

It is noteworthy that *M. ulcerans* subsp. *shinshuense* was identified in all of the isolates from Japanese patients diagnosed with BU. *M. ulcerans* subsp. *shinshuense*, not *M. ulcerans*, could be the primary etiological agent of BU in eastern Asia. It has been reported that the STPK gene was not amplified from the isolate of a BU patient in China (26). While there might be a taxonomical reason, this isolate was finally classified as *M. ulcerans* (4). A more precise genotypic examination might have revealed this to be a case of *M. ulcerans* subsp. *shinshuense* infection. If so, this finding would suggest that *M. ulcerans* subsp. *shinshuense* is distributed not only in Japan, but also in other areas of eastern Asia. Thorough field work and increased vigilance on the part of dermatologists and physicians are needed to determine the predominant cause of BU in eastern Asia. Because disease severity and susceptibility to antibacterial drugs are significantly different for *M. ulcerans* versus *M. ulcerans* subsp. *shinshuense*, they must be identified and distinguished in clinical settings.

The Japanese *M. ulcerans* subsp. *shinshuense* isolates and the Chinese strain of *M. ulcerans* presumably belong to the same cluster, based on genetic analyses such as microarray-based comparative genomic hybridization (9) and comparative sequence analysis of polymorphic variable-number tandem repeats (VNTR) (27). Their genomes were distinctly different from those of *M. ulcerans* strains that originated in other geographic regions. However, one of the VNTR loci can be used to distinguish between the Chinese and Japanese strains (1). Pidot et al. described the clear difference between the two strains by analyzing virulent plasmid genes and the resulting mycolactone production, noting that the Japanese strain produces mycolactone A/B, while the Chinese strain produces a unique mycolactone D (19). Further study is needed to elucidate the evolution and distribution of *M. ulcerans*, and its relation to *M. ulcerans* subsp. *shinshuense*, in Asia.

It is notable that most of the biochemical characteristics (Table 5) and drug susceptibilities (Table 6) of the isolates were the same as those found in a previous report (22), with the exception of the urease test. Interestingly, the Japanese *M. ulcerans* subsp. *shinshuense* isolates, the Chinese strain of *M. ulcerans*, and the related species *M. marinum* were all urease positive, though other strains of *M. ulcerans* originating from Ghana and Australia were urease negative. The urease test is a simple method with clear results that would be useful in distinguishing between *M. ulcerans* and *M. ulcerans* subsp. *shinshuense*.

Clinical manifestation of BU in Japan was essentially similar to that of BU in other countries, but distinct differences in management were observed. Ulcerated areas were usually smaller for Japanese (Fig. 3) than for African patients; how-

ever, the Japanese patients received both surgery and a large array of antimycobacterial drugs (Table 7). In addition, in Africa, most patients who had lesions with cross-sectional diameters of ≤10 cm showed excellent healing without surgery (17). Although the *in vitro* susceptibilities of the Japanese isolates to streptomycin, kanamycin, and clarithromycin are higher than those of the *M. ulcerans* strains from West Africa (Table 6), treatment has been fairly aggressive in Japan. It is speculated that because the majority of doctors and patients in Japan have not experienced and cannot recognize Buruli ulcer disease, they might fear the progression and recurrence of disease. Especially when patients complain of pain (9 patients in this study [47%] experienced pain [Fig. 4]), their doctors and family members are willing to initiate aggressive treatment, even in the absence of an immunodeficiency risk factor. Public information campaigns about the disease are needed, as is the establishment of guidelines for the treatment of Buruli ulcer in Japan. Clarification of the mode of transmission is also important. However, the occurrence of cases has been very sporadic, and none could be linked to an aquatic environment. Thus, the source and route of the infection remain unclear.

ACKNOWLEDGMENTS

This work was supported in part by a Grant-in-Aid for Research on Emerging and Re-emerging Infectious Diseases from the Ministry of Health, Labor, and Welfare of Japan (to Y.H., M.M., and N.I.), by a Grant-in-Aid for Scientific Research (C) from the Ministry of Education, Culture, Sports, Science and Technology of Japan (to Y.H.), and by a Grant-in-Aid for Scientific Research (C) from the Japan Society for the Promotion of Science (to K.N.).

REFERENCES

1. **Ablordey, A., et al.** 2005. Comparative nucleotide sequence analysis of polymorphic variable number tandem repeat loci in *Mycobacterium ulcerans*. J. Clin. Microbiol. **43:**5281–5284.
2. **Alsop, D. G.** 1972. The Bairnsdale ulcer. Aust. N. Z. J. Surg. **41:**317–319.
3. **Clancey, J. K., O. G. Dodge, H. F. Lunn, and M. L. Oduori.** 1961. Mycobacterial skin ulcers in Uganda. Lancet **ii:**951–954.
4. **Faber, W. R., et al.** 2000. First reported case of *Mycobacterium ulcerans* infection in a patient from China. Trans. R. Soc. Trop. Med. Hyg. **94:**277–279.
5. **Fenner, F.** 1951. The significance of the incubation period in infectious diseases. Med. J. Aust. **2:**813–818.
6. **Funakoshi, T., et al.** 2009. Intractable ulcer caused by *Mycobacterium shinshuense*: successful identification of mycobacterium strain by 16S ribosomal RNA 3′-end sequencing. Clin. Exp. Dermatol. **34:**e712–e715.
7. **Imada, H., et al.** 2008. Cutaneous ulcer of a right olecranon due to *Mycobacterium shinshuense*; a case report. Seikeigeka **59:**1440–1445. (In Japanese.)
8. **Kaminuma, E., et al.** 2010. DDBJ launches a new archive database with analytical tools for next-generation sequence data. Nucleic Acids Res. **38**(Database issue):D33–D38.
9. **Käser, M., et al.** 2007. Evolution of two distinct phylogenetic lineages of the emerging human pathogen *Mycobacterium ulcerans*. BMC Evol. Biol. **7:**177.
10. **Kazumi, Y., et al.** 2004. *Mycobacterium shinshuense* isolated from cutaneous ulcer lesion of right lower extremity in a 37-year-old woman. Kekkaku **79:**437–441. (In Japanese.)
11. **Kim, B.-J., et al.** 1999. Identification of mycobacterial species by comparative sequence analysis of the RNA polymerase gene (*rpoB*). J. Clin. Microbiol. **37:**1714–1720.
12. **Kondo, M., et al.** 2009. Leg ulcer caused by *Mycobacterium ulcerans* ssp. *shinshuense* infection. Int. J. Dermatol. **48:**1330–1333.
13. **Kusunoki, S., et al.** 1991. Application of colorimetric microdilution plate hybridization for rapid genetic identification of 22 *Mycobacterium* species. J. Clin. Microbiol. **29:**1596–1603.
14. **MacCallum, P., J. C. Tolhurst, G. Buckle, and H. I. Sissons.** 1948. A new mycobacterial infection in man. I. Clinical aspects. II. Experimental investigations in laboratory animals. III. Pathology of the experimental lesions in the rat. IV. Cultivation of the new mycobacterium. J. Pathol. Bacteriol. **60:**93–122.
15. **Mikoshiba, H., et al.** 1982. A case of atypical mycobacteriosis due to *Mycobacterium ulcerans*-like organism. Nihon Hifukagakkaizassi **92:**557–565. (In Japanese.)
16. **Nakanaga, K., et al.** 2007. "*Mycobacterium ulcerans* subsp. *shinshuense*" isolated from a skin ulcer lesion: identification based on 16S rRNA gene sequencing. J. Clin. Microbiol. **45:**3840–3843.
17. **Nienhuis, W. A., et al.** 2010. Antimicrobial treatment for early, limited *Mycobacterium ulcerans* infection: a randomized controlled trial. Lancet **375:**664–672.
18. **Phillips, R. C., et al.** 2005. Sensitivity of PCR targeting the IS*2404* insertion sequence of *Mycobacterium ulcerans* in an assay using punch biopsy specimens for diagnosis of Buruli ulcer. J. Clin. Microbiol. **43:**3650–3656.
19. **Pidot, S. J., et al.** 2008. Deciphering the genetic basis for polyketide variation among mycobacteria producing mycolactones. BMC Genomics **9:**462.
20. **Portaels, F., et al.** 1996. Variability in 3′ end of 16S rRNA sequence of *Mycobacterium ulcerans* is related to geographic origin of isolates. J. Clin. Microbiol. **34:**962–965.
21. **Portaels, F., M. T. Silva, and W. M. Meyers.** 2009. Buruli ulcer. Clin. Dermatol. **27:**291–305.
22. **Portaels, F., P. Johnson, and W. M. Meyers (ed.).** April 2001. Buruli ulcer: diagnosis of *Mycobacterium ulcerans* disease. A manual for health care providers. World Health Organization, Geneva, Switzerland. http://whqlibdoc.who.int/hq/2001/WHO_CDS_CPE_GBUI_2001.4.pdf.
23. **Roth, A., et al.** 1998. Differentiation of phylogenetically related slowly growing mycobacteria based on 16S–23S rRNA gene internal transcribed spacer sequences. J. Clin. Microbiol. **36:**139–147.
24. **Springer, B., et al.** 1996. Isolation and characterization of a unique group of slowly growing mycobacteria: description of *Mycobacterium lentiflavum* sp. nov. J. Clin. Microbiol. **34:**1100–1107.
25. **Stinear, T. P., et al.** 2004. Giant plasmid-encoded polyketide synthases produce the macrolide toxin of *Mycobacterium ulcerans*. Proc. Natl. Acad. Sci. U. S. A. **101:**1345–1349.
26. **Stinear, T. P., et al.** 2005. Common evolutionary origin for the unstable virulence plasmid pMUM found in geographically diverse strains of *Mycobacterium* ulcerans. J. Bacteriol. **187:**1668–1676.
27. **Stragier, P., A. Ablordey, L. Durnez, and F. Portaels.** 2007. VNTR analysis differentiates *Mycobacterium ulcerans* and IS*2404* positive mycobacteria. Syst. Appl. Microbiol. **30:**525–530.
28. **Suzuki, S., et al.** 2008. Skin ulcer caused by '*Mycobacterium ulcerans* subsp. *shinshuense* ' infection. Hifubyou Shinryo **30:**145–148. (In Japanese.)
29. **Tamura, K., J. Dudley, M. Nei, and S. Kumar.** 2007. MEGA4: molecular evolutionary genetic analysis (MEGA) software version 4.0. Mol. Biol. Evol. **24:**1596–1599.
30. **Telenti, A., et al.** 1993. Rapid identification of mycobacteria to the species level by polymerase chain reaction and restriction enzyme analysis. J. Clin. Microbiol. **31:**175–178.
31. **Tsukamura, M., and H. Mikoshiba.** 1989. A taxonomic study on a mycobacterium which caused skin ulcer in a Japanese girl and resembled *Mycobacterium ulcerans*. Kekkaku **64:**691–697. (In Japanese.)
32. **Uganda Buruli Group.** 1971. Epidemiology of *Mycobacterium ulcerans* infection (Buruli ulcer) at Kinyara, Uganda. Trans. R. Soc. Trop. Med. Hyg. **65:**763–775.
33. **Wallace, R. J., Jr, D. R. Nash, L. C. Steele, and V. Steingrube.** 1986. Susceptibility testing of slowly growing mycobacteria by a microdilution MIC method with 7H9 broth. J. Clin. Microbiol. **24:**976–981.
34. **Walsh, D. S., F. Portaels, and W. M. Meyers.** 2011. Buruli ulcer: advances in understanding *Mycobacterium ulcerans* infection. Dermatol. Clin. **29:**1–8.
35. **Watanabe, T., et al.** 2010. Buruli ulcer caused by "*Mycobacterium ulcerans* subsp. *shinshuense*." Eur. J. Dermatol. **20:**809–810.
36. **World Health Organization.** October 2004. Provisional guidance on the role of specific antibiotics in the management of *Mycobacterium ulcerans* disease (Buruli ulcer). World Health Organization, Geneva, Switzerland. http://whqlibdoc.who.int/hq/2004/WHO_CD5_CPE_GBUI_2004.10.pdf..

JOURNAL OF BACTERIOLOGY, Oct. 2011, p. 5766–5774 Vol. 193, No. 20
0021-9193/11/$12.00 doi:10.1128/JB.05412-11

Structure and Host Recognition of Serotype 13 Glycopeptidolipid from *Mycobacterium intracellulare*▽†

Takashi Naka,[1,2]‡ Noboru Nakata,[3]‡ Shinji Maeda,[4]‡ Reina Yamamoto,[1,5] Matsumi Doe,[6] Seiko Mizuno,[1,5] Mamiko Niki,[1] Kazuo Kobayashi,[7] Hisashi Ogura,[1,8] Masahiko Makino,[3] and Nagatoshi Fujiwara[1]*

Departments of Bacteriology[1] and Virology,[8] Osaka City University Graduate School of Medicine, Osaka 545-8585, Japan; MBR Co. Ltd., Osaka 560-8552, Japan[2]; Department of Mycobacteriology, Leprosy Research Center, National Institute of Infectious Diseases, Tokyo 189-0002, Japan[3]; Molecular Epidemiology Division, Mycobacterium Reference Center, The Research Institute of Tuberculosis, Japan Anti-Tuberculosis Association, Tokyo 204-8533, Japan[4]; Department of Development Nourishment, Faculty of Human Development, Soai University, Osaka 559-0003, Japan[5]; Department of Chemistry, Graduate School of Science, Osaka City University, Osaka 558-8585, Japan[6]; and Department of Immunology, National Institute of Infectious Diseases, Tokyo 162-8640, Japan[7]

Received 31 May 2011/Accepted 31 July 2011

The *Mycobacterium avium-M. intracellulare* complex (MAIC) is divided into 28 serotypes by a species-specific glycopeptidolipid (GPL). Previously, we clarified the structures of serotype 7 GPL and two methyltransferase genes (*orfA* and *orfB*) in serotype 12 GPL. This study elucidated the chemical structure, biosynthesis gene, and host innate immune response of serotype 13 GPL. The oligosaccharide (OSE) structure of serotype 13 GPL was determined to be 4-2′-hydroxypropanoyl-amido-4,6-dideoxy-β-hexose-(1→3)-4-*O*-methyl-α-L-rhamnose-(1→3)-α-L-rhamnose-(1→3)-α-L-rhamnose-(1→2)-α-L-6-deoxy-talose by using chromatography, mass spectrometry, and nuclear magnetic resonance (NMR) analyses. The structure of the serotype 13 GPL was different from those of serotype 7 and 12 GPLs only in *O*-methylations. We found a relationship between the structure and biosynthesis gene cluster. *M. intracellulare* serotypes 12 and 13 have a 1.95-kb *orfA-orfB* gene responsible for 3-*O*-methylation at the terminal hexose, *orfB*, and 4-*O*-methylation at the rhamnose next to the terminal hexose, *orfA*. The serotype 13 *orfB* had a nonfunctional one-base missense mutation that modifies serotype 12 GPL to serotype 13 GPL. Moreover, the native serotype 13 GPL was multiacetylated and recognized via Toll-like receptor 2. The findings presented here imply that serotypes 7, 12, and 13 are phylogenetically related and confirm that acetylation of the GPL is necessary for host recognition. This study will promote better understanding of the structure-function relationships of GPLs and may open a new avenue for the prevention of MAIC infections.

The increase of drug-resistant mycobacteria and the number of immunocompromised hosts including the HIV epidemic are important problems. The *Mycobacterium avium-M. intracellulare* complex (MAIC) is distributed ubiquitously in the environment and is the most common isolate of nontuberculous mycobacteria, which are now one of the most important environmental pathogen-disseminated infectious agents in both immunocompromised and immunocompetent hosts (26, 31, 39).

The most characteristic feature of mycobacteria is richness in lipids. These hydrophobic cell wall components contribute to the surface properties and are considered to play important roles in their pathogenesis through the host immune responses (8, 17). MAIC expresses a glycopeptidolipid (GPL) as one of the representative lipid components. Structurally, the GPL is composed of two parts, a common tetrapeptido-amino alcohol core and a serotype-specific oligosaccharide (OSE) elongated from 6-deoxy-talose (6-d-Tal). D-Phenylalanine-D-*allo*-threonine-D-alanine-L-alaninol (D-Phe-D-*allo*-Thr-D-Ala-L-alaninol), which is modified with an amido-linked 3-hydroxy or 3-methoxy C_{26}-C_{34} fatty acid at the *N* terminus of D-Phe, and D-*allo*-Thr and terminal L-alaninol are further linked to a 6-d-Tal and 3,4-di-*O*-methyl rhamnose (3,4-di-*O*-Me-Rha), respectively. This portion is called the serotype-nonspecific GPL (apolar GPL). Serotype-specific GPLs (polar GPLs) are produced by extending individual OSE residues from the 6-d-Tal. MAIC species are divided into 28 serotypes by serological reaction and distinctive patterns of polar GPLs on thin-layer chromatography (TLC) (7, 38). The GPL is considered to play crucial roles in the physiology of the bacteria and the host responses to MAIC infection. Several biological and immunological functions of GPLs have been reported (9, 34), but the roles of GPLs are not fully elucidated. Recently, several genes involved in GPL biosynthesis have been characterized (10, 29). To better understand the biological functions and significance of GPLs, we need to clarify the structure and biosynthetic pathways of GPLs.

The chemical structures of only 16 GPLs have been defined (9). Recently, we determined the structures of the serotype 7 and 16 GPLs and identified the gene clusters completing the OSE biosynthesis (13, 14). In addition, two methyltransferase genes of serotype 7- and 12-specific GPL biosynthesis were

* Corresponding author. Mailing address: Department of Bacteriology, Osaka City University Graduate School of Medicine, 1-4-3 Asahi-machi, Abeno-ku, Osaka 545-8585, Japan. Phone: 81 6 6645 3746. Fax: 81 6 6645 3747. E-mail: fujiwara@med.osaka-cu.ac.jp.

† Supplemental material for this article may be found at http://jb.asm.org/.

‡ These authors contributed equally to this work.

▽ Published ahead of print on 19 August 2011.

characterized (30). In this process, we found that the structure of the serotype 13 GPL is close to that of the serotype 7 and 12 GPLs. In epidemiological serotyping, Tsang et al. (37) showed that clinical isolates of serotypes 7, 12, and 13 were found in around 10% of non-AIDS patients. However, it was difficult to distinguish serotypes 7, 12, and 13 by only serological and chromatographic techniques because of their structural similarity. The phylogeny of some MAIC strains based on GPL biosynthesis genes has been reported (23). In this study, the complete structure of the serotype 13 GPL was determined, and the genetic relationship between the serotype 7, 12, and 13 GPL biosynthesis was clarified. Moreover, the host innate immune recognition of antigenic serotype 13 GPL and the importance of structural modification were shown. We discuss the phylogeny of MAIC strains on the basis of these GPL biosynthesis genes and the relationship between GPL structure and immunogenicity.

MATERIALS AND METHODS

Bacterial strains and preparation of GPL. *M. intracellulare* serotype 13 (ATCC 35769, ATCC 25122), serotype 7 (ATCC 35847), and serotype 12 (ATCC 35762) strains were purchased from the American Type Culture Collection (Manassas, VA). The GPL preparation was performed as described previously (14, 18). Each strain of *M. intracellulare* was grown on Middlebrook 7H11 agar (Difco Laboratories, Detroit, MI) with 0.5% glycerol and 10% Middlebrook oleic acid-albumin-dextrose-catalase (OADC) enrichment (Difco) at 37°C for 2 to 3 weeks. The heat-killed bacteria were sonicated, and crude lipids were extracted with chloroform-methanol (2:1 [vol/vol]). The crude lipids were hydrolyzed with 0.2 N sodium hydroxide in methanol at 37°C for 2 h, followed by neutralization with 6 N hydrochloric acid. Alkaline-stable lipids were partitioned by a two-layer system with chloroform-methanol (2:1 [vol/vol]) and water. The organic phase was evaporated and precipitated with acetone to remove any acetone-insoluble components. The supernatant was washed (chloroform-methanol, 95:5 [vol/vol]) and eluted (chloroform-methanol, 1:1 [vol/vol]) with a Sep-Pak silica cartridge (Waters Corporation, Milford, MA) for partial purification. The GPL was completely purified by preparative TLC of Silicagel G (Uniplate; 20 by 20 cm, 250 μm; Analtech, Inc., Newark, DE). The TLC plate was developed with chloroform-methanol-water (65:25:4 and 60:16:2 [vol/vol/vol]), until a single spot was obtained. The TLC plate was sprayed with 20% sulfuric acid in ethanol and was charred at 180°C for 3 min. The GPL was detected as a brownish-yellow spot. To recover the GPL, the TLC plate was exposed to iodine vapor, and the GPL spot was marked. The silica gels of the GPL spot were scraped off, and the GPL was eluted with chloroform-methanol (2:1 [vol/vol]). The native GPL was purified by the same method as the alkaline-stable GPL, omitting the hydrolysis with 0.2 N sodium hydroxide.

Preparation of OSE moiety. β-Elimination of the GPL was performed with alkaline borohydride, and the OSE elongated from D-*allo*-Thr was released (14, 18). The GPL was stirred in a solution of equal volumes of ethanol and 10 mg/ml sodium borodeuteride in 0.5 N sodium hydroxide at 60°C for 16 h. The reaction mixture was decationized with Dowex 50W X8 beads (Dow Chemical Company, Midland, MI) and evaporated under nitrogen to remove boric acid. After partition into two layers of chloroform-methanol (2:1 [vol/vol]) and water, the upper aqueous phase was recovered and evaporated, and the OSE was purified as an oligoglycosyl alditol.

MALDI-TOF MS and MALDI-TOF MS/MS. The molecular species of the intact GPL was determined by the matrix-assisted laser desorption ionization–time of flight mass spectrometry (MALDI-TOF MS) with an Ultraflex II (Bruker Daltonics, Billerica, MA). One microgram of the GPL-dissolved chloroform-methanol (2:1 [vol/vol]) was applied to the target plate, and 1 μl of 10 mg/ml 2,5-dihydroxybenzoic acid in chloroform-methanol (1:1 [vol/vol]) was added as a matrix. The intact GPL was analyzed in the Reflectron mode with an accelerating voltage operating in positive mode at 20 kV (4). Then, the fragment pattern of the OSE was analyzed with the MALDI-TOF MS/MS mode. The OSE and 10 mg/ml 2,5-dihydroxybenzoic acid was dissolved in ethanol-water (3:7 [vol/vol]) and applied to the target plate according to the method for intact GPL.

GC/MS of carbohydrates. To determine the glycosyl composition and linkage position, gas chromatography/mass spectrometry (GC/MS) of partially methylated alditol acetate derivatives was performed. Perdeuteromethylation was conducted by the modified procedure of Hakomori (14, 15). The OSE was dissolved with a mixture of dimethyl sulfoxide and sodium hydroxide, followed by the addition of deuteromethyl iodide. After stirring at room temperature for 15 min, the reaction mixture was separated by a two-layer system of water and chloroform. The chloroform-containing perdeuteromethylated OSE layer was collected, washed with water two times, and evaporated completely. Partially deuteromethylated alditol acetate derivatives were prepared from perdeuteromethylated OSE by hydrolysis with 2 N trifluoroacetic acid at 120°C for 2 h, reduction with 10 mg/ml sodium borodeuteride at 25°C for 2 h, and acetylation with acetic anhydride at 100°C for 1 h (14, 19). GC/MS was performed using a benchtop ion trap mass spectrometer (GCMS-QP2010 Plus; Shimadzu Corp., Kyoto, Japan) equipped with a fused capillary column (SP-2380 and Equity-1; 30 m, 0.25-mm inner diameter [ID]; Supelco, Bellefonte, PA). Helium was used

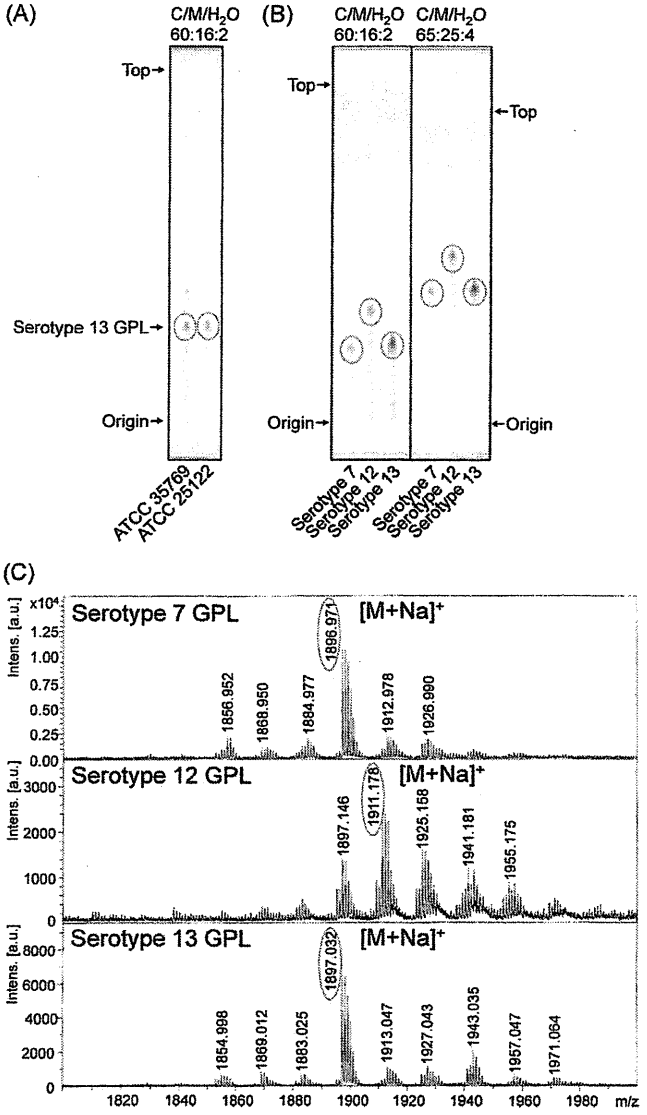

FIG. 1. TLC patterns and MALDI-TOF MS spectra of serotype 7, 12, and 13 GPLs. (A and B) The alkaline-stable lipids derived from *M. intracellulare* serotype 13 ATCC 35769 and ATCC 25122 (A) and the purified serotype 7, 12, and 13 GPLs (B) were developed on TLC plates with solvent systems of chloroform-methanol-water (60:16:2 and 65:25:4 [vol/vol/vol]). (C) The MALDI-TOF MS spectra of serotype 7, 12, and 13 GPLs were acquired using 10 mg/ml 2,5-dihydroxybenzoic acid in chloroform-methanol (1:1 [vol/vol]) as a matrix, and the molecular ions were detected as $[M+Na]^+$ in positive mode. Intens., intensity; a.u., arbitrary units.

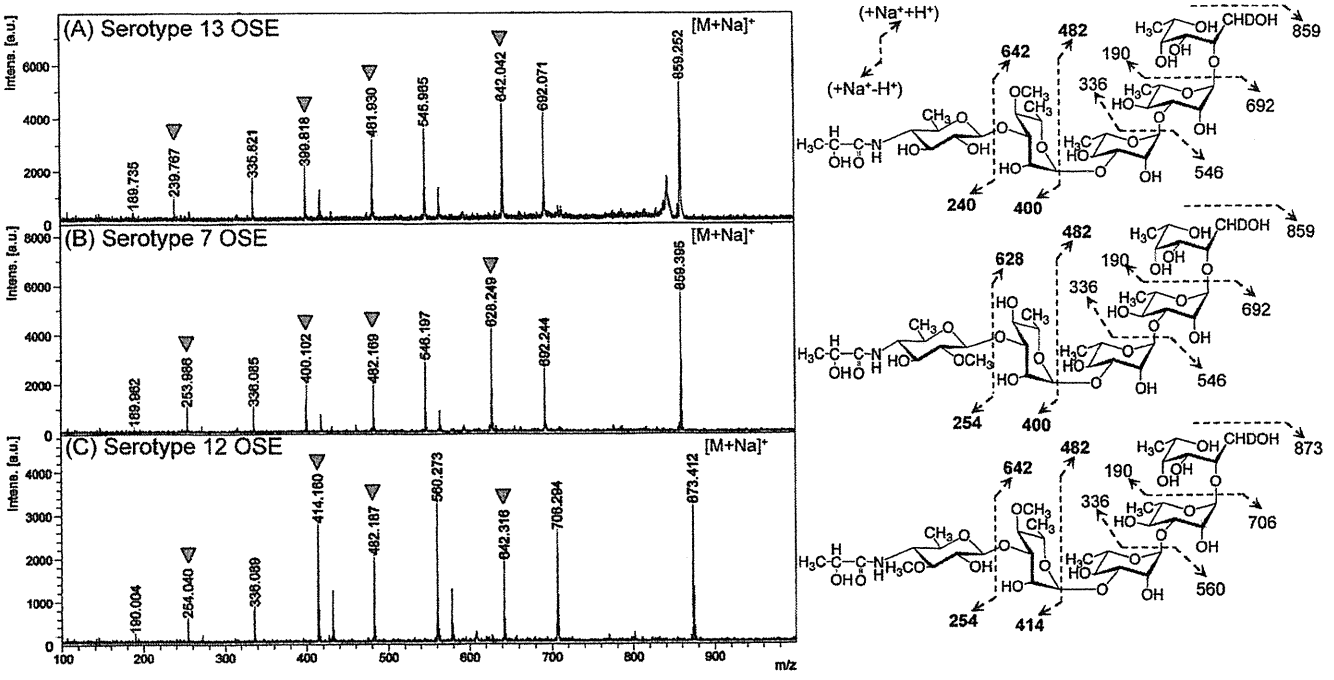

FIG. 2. MALDI-TOF MS/MS spectra of serotype 13, 7, and 12 OSEs (A, B, and C, respectively). The fragment ions by each glycosyl cleavage were detected, and the assigned fragment patterns are illustrated. Arrowheads indicate the characteristic mass numbers of the serotype 13, 7, and 12 OSEs. The matrix was 10 mg/ml 2,5-dihydroxybenzoic acid in ethanol-water (3:7 [vol/vol]), and it was performed in the MS/MS mode. Intens., intensity; a.u., arbitrary units.

as the carrier gas, and the flow rate was 1 ml/min. The temperature program for alditol acetate derivatives was started at 60°C, increased 40°C/min to 220°C, and held for 15 min, followed by an increase of 10°C/min to 260°C and holding for 10 min. The molecular separator and ion source energies were 70 eV, and the accelerating voltage was 8 kV.

NMR of GPL. The OSE was dissolved in deuterium oxide. To define the anomeric configurations of each glycosyl residue, ^{1}H and ^{13}C nuclear magnetic resonance (NMR) was employed. Both homonuclear correlation spectrometry (COSY) and ^{1}H-detected [^{1}H, ^{13}C] heteronuclear multiple-quantum correlation (HMQC) were recorded with a Bruker AVANCE-600 (Bruker BioSpin Corp. Billerica, MA), as described previously (14, 18). Ten microliters of acetone was added to the sample, and its chemical shift values, 2.04 ppm (proton) and 29.8 ppm (carbon), were used as internal controls.

Sequencing of *orfA-orfB* region of *M. intracellulare* serotype 13. PCR was used to amplify the *orfA-orfB* region (30) of *M. intracellulare* serotype 13 (ATCC 35769 and ATCC 25122), using primers *orfA*-F (5′-GCGGATCCAGTGTGCAGACG AGCGGAACT-3′), *orfA*-R (5′-GCGAATTCTTATCGAGAAAAAATAAAA G-3′), *orfB*-F (5′-GCGGATCCACTGCTAGACT CCGCCACCAT-3′), and *orfB*-R (5′-GCGAATTCCTACACCTTCACGGCGAGTC-3′). The amplified fragment was sequenced using a BigDye Terminator cycle sequencing kit, version 3.1 (Applied Biosystems, Foster City, CA), and a sequence analyzer (ABI3130xl; Applied Biosystems).

Transformation of *M. intracellulare* serotype 13 strain with serotype 12 *orfB*. The *orfB* fragments from serotype 12 (sero12-*orfB*) and serotype 13 (sero13-*orfB*) strains were amplified and cloned into pVV16, an expression plasmid vector for mycobacteria, downstream of the hsp60 promoter. *M. intracellulare* serotype 13 ATCC 35769 was transformed with pVV16-sero12-*orfB* and pVV16-sero13-*orfB* by electroporation, and hygromycin- and kanamycin-resistant colonies were isolated. Alkaline-stable lipids were prepared from heat-killed bacteria, and productive GPLs were identified by TLC, MALDI-TOF MS, MALDI-TOF MS/MS, and GC/MS.

Host recognition of native and alkaline-treated serotype 13 GPLs. The host recognition of GPLs was estimated by activations of HEK-blue-2 and -4 cells (InvivoGen, San Diego, CA). HEK-blue-2 and -4 cells are HEK293 cells stably transfected with multiple genes for recognition of Toll-like receptor 2 (TLR2) and TLR4 (including the coreceptors MD2 and CD14). In addition, HEK-blue-2 and -4 cells stably express an optimized alkaline phosphatase gene engineered to be secreted (sAP) and placed under the control of a promoter inducible by several transcription factors, such as NF-κB and alkaline phosphatase-1. HEK-blue-2 and -4 cells were seeded at a concentration of 2×10^5 cells/ml in 96-well flat-bottom tissue culture plates and incubated with Dulbecco's modified Eagle's medium (DMEM) containing 10% fetal bovine serum (FBS) at 37°C in an atmosphere of 5% CO_2 for 3 days. The adherent HEK-blue-2 and -4 cells were stimulated by native and alkaline-treated serotype 13 GPLs. After 24 h of incubation, NF-κB activation was assayed by the levels of sAP in the supernatant. The sAP was measured in duplicate using QUANTI-Blue (InvivoGen) according to the manufacturer's instructions. As positive controls, we used lipopolysaccharide (LPS) from *Escherichia coli* 055:B5 (Sigma-Aldrich, St. Louis, MO) for TLR4 and Pam3CSK4 (InvivoGen) for TLR2. Two independent experiments were performed.

Nucleotide sequence accession number. The nucleotide sequence reported here has been deposited in the NCBI GenBank database under accession number AB557690.

RESULTS

Purification and molecular weight of intact GPL. The serotype 13 GPLs from *M. intracellulare* ATCC 35769 and 25122 were detected as spots on TLC plates and showed the same R_f value (Fig. 1A). Because serotype 13 GPL was predicted to be very close structurally to the serotype 7 and 12 GPLs, the R_f values were compared on TLC plates developed with two different chloroform-methanol-water solvent systems (65:25:4 and 60:16:2 [vol/vol/vol]), respectively. Interestingly, the R_f value of the serotype 13 GPL was lower than that of the serotype 12 GPL and almost the same as that of the serotype 7 GPL in both developing systems (Fig. 1B). The intact molecular weight of each GPL was determined. The MALDI-TOF MS spectrum of the serotype 13 GPL showed *m/z* 1,897 for $[M+Na]^+$ as the main molecular ion in positive mode (Fig.

1C). This mass number is identical to that of the serotype 7 GPL ($[M+Na]^+$: 1,897) and 14 atomic mass units lower than that of the serotype 12 GPL ($[M+Na]^+$: 1,911).

Glycosyl sequence of serotype 13 OSE. To determine the glycosyl sequence of the OSE, MALDI-TOF MS/MS of the oligoglycosyl alditol from serotype 13 OSE was performed. The spectrum afforded the molecular ion $[M+Na]^+$ at *m/z* 859, together with the characteristic mass increments in the series of glycosyloxonium ions formed on fragmentation at *m/z* 240, 400, 546, and 692 from the *N*-acylated Hex to 6-d-Tal, and at *m/z* 190, 336, 482, and 642 from 6-d-Tal to *N*-acylated Hex (Fig. 2A). In comparison, the fragment patterns of the cleaved terminal *N*-acylated Hex of the OSEs were *m/z* 254 and 628 in serotype 7 and *m/z* 254 and 642 in serotype 12, and those next to the terminal Hex were *m/z* 400 and 482 in serotype 7 and *m/z* 414 and 482 in serotype 12 (Fig. 2B and C). Together with the intact molecular weight of each GPL (Fig. 1B), these results strongly implied that serotype 13 GPL has no *O*-methyl group in the terminal *N*-acylated Hex but does have an *O*-methyl group added to the Rha next to the terminal Hex.

Carbohydrate composition and linkage analyses. GC/MS analysis of the perdeuteromethylated alditol acetate derivative from serotype 13 OSE was performed to determine the glycosyl composition. The total ion chromatography (TIC) of the GC/MS spectrum of serotype 13 GPL derivatives was compared to those of serotype 7 and 12 GPL derivatives (Fig. 3A). Previous reports showed that the carbohydrate compositions of the serotype 7 GPL were 6-d-Tal, Rha, and 4-2′-hydroxypropanoyl-amido-3,6-dideoxy-2-*O*-Me-Hex, and those of the serotype 12 GPL were 6-d-Tal, Rha, 4-*O*-Me-Rha, and 4-2′-hydroxypropanoyl-amido-3,6-dideoxy-3-*O*-Me-Hex (5, 13). Comparison of the retention times and mass spectra of GC/MS determined that serotype 13 GPL was composed of 6-d-Tal, Rha, 4-*O*-Me-Rha, and another terminal *N*-acylated Hex. As shown in Fig. 3B, the perdeuteromethylated alditol acetate derivative of the terminal *N*-acylated Hex was assigned to 2,3-di-*O*-deuteromethyl-1,5-di-*O*-acetyl-4-2′-*O*-deuteromethyl-propanoyl-deuteromethylamido-4,6-dideoxy-hexitol from the fragment pattern (*m/z* 62, 108, 121, 168, 209, 222, 269, and 303). These results confirmed that the *O*-methyl group was deleted from the terminal *N*-acylated Hex and added to the C-4 position at Rha next to the terminal Hex. Taken together, these results established the sequence and linkage arrangement of 4-2′-hydroxypropanoyl-amido-4,6-dideoxy-Hex-(1→3)-4-*O*-Me-Rha-(1→3)-L-Rha-(1→3)-L-Rha-(1→2)-6-d-Tal exclusively.

NMR analysis of serotype 13 OSE. The ^1H NMR and ^1H-^1H homonuclear COSY analyses of the OSE derived from the serotype 13 GPL revealed four distinct anomeric protons with corresponding H1-H2 cross-peaks in the low-field region at δ4.88, 4.71, 4.97 (J_{1-2} = 1 to 2 Hz, indicative of α-anomers), and 4.52 (a doublet, J_{1-2} = 7.9 Hz, indicative of a β-hexosyl unit). When further analyzed by ^1H-detected [^1H-^{13}C] two-dimensional HMQC, the anomeric protons resonating at δ4.88, 4.71, 4.97, and 4.52 had C-1s resonating at δ102.10, 93.50, 94.00, and 103.40, respectively. The J_{CH} values for each of these protons were calculated to be 170, 170, 171, and 161 Hz by measurement of the inverse-detection nondecoupled two-dimensional HMQC (see Fig. S1 and Table S1 in the supplemental material). It was concluded that two Rha and 4-*O*-Me Rha were α-anomers and that the terminal *N*-acylated Hex was a β configuration.

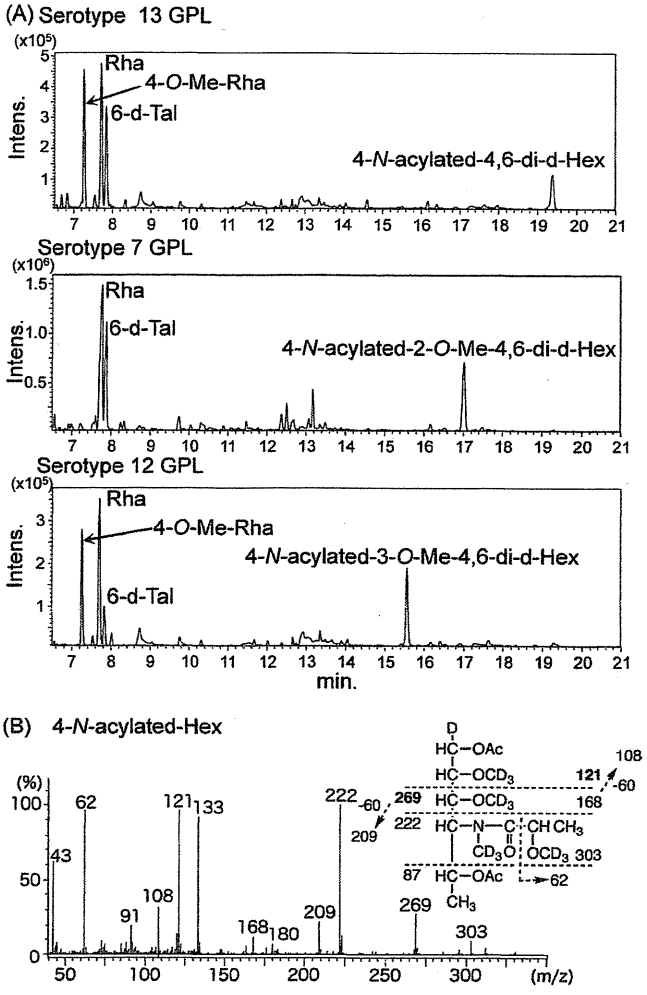

FIG. 3. Assignment of glycosyl composition of OSEs in serotype 13 GPL. (A) Total ion chromatogram of the alditol acetate derivatives from serotype 13 compared to those of serotype 7 and 12 GPLs. A fused SP-2380 capillary column was used as the GC column. The temperature program for alditol acetate derivatives was started at 60°C, increased to 40°C/min to 220°C, and held for 15 min, followed by an increase of 10°C/min to 260°C and holding for 10 min. (B) GC/MS spectrum of the perdeuteromethylated alditol acetate derivative from the terminal Hex in serotype 13 GPL. The pattern of prominent fragment ions is illustrated. A fused Equity-1 capillary column was used as the GC column. Ac, CH_3CO.

Nucleotide sequence of *orfA-orfB* region of *M. intracellulare* serotype 13. The present study demonstrated that the difference between the chemical structures of the serotype 13 GPL and serotype 7 and 12 GPLs was whether the *O*-methyl group in the terminal *N*-acylated Hex and the next Rha were present or not. We confirmed the genetic basis of these *O*-methylations. Our previous study clarified three unique open reading frames (ORFs) for methyltransferase, named *orf2*, derived from *M. intracellulare* serotype 7, and *orfA* and *orfB*, from *M. intracellulare* serotype 12 (13, 30). *orfA* and *orfB* in *M. intracellulare* serotype 12 are responsible for 4-*O*-methylation of the Rha next to the terminal Hex and 3-*O*-methylation of the

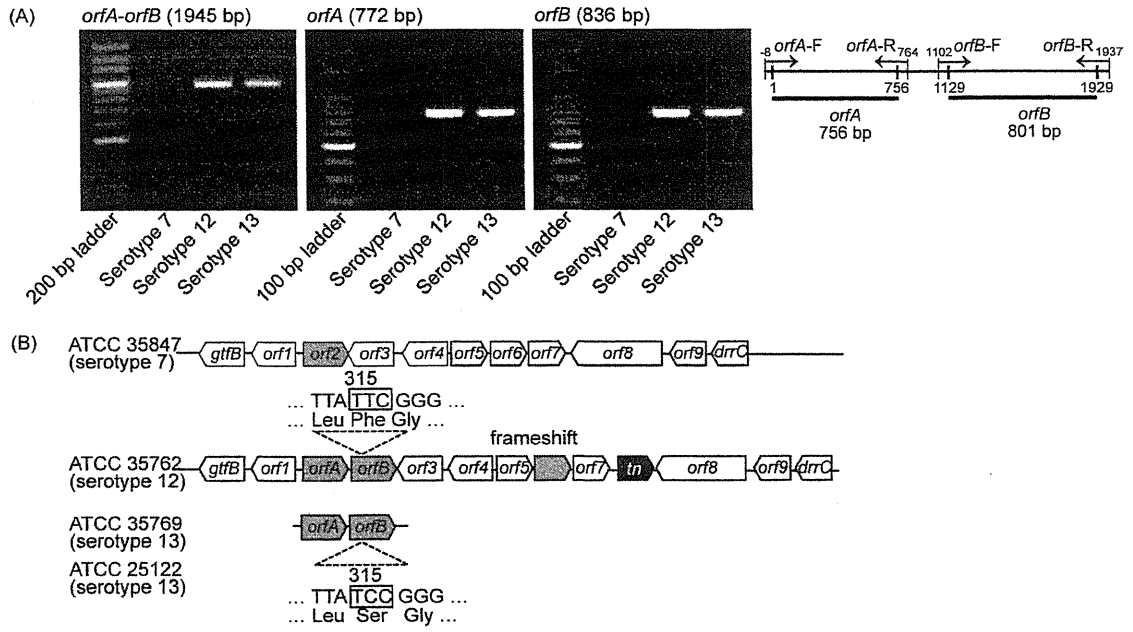

FIG. 4. Detection of *orfA-orfB* regions and comparison of genetic maps of GPL biosynthetic cluster. (A) PCR was performed to amplify the *orfA-orfB* regions of *M. intracellulare* serotype 7, 12, and 13 strains. The primers and the amplified regions are indicated. (B) *M. intracellulare* serotype 7 ATCC 35847 and serotype 12 ATCC 35762 were sequenced in our previous work (13, 30). *M. intracellulare* serotype 13 ATCC 35769 and ATCC 25122 were sequenced in this study. The missense mutation of *orfA-orfB* regions is indicated.

terminal Hex, respectively. Therefore, we examined whether or not *M. intracellulare* serotype 13 has these ORFs. First, comparison of the *gtfB-drrC* gene cluster in *M. intracellulare* serotype 7 and 12 strains implied that *orf2* in *M. intracellulare* serotype 7 replaced *orfA-orfB* in *M. intracellulare* serotype 12. We amplified the *orfA-orfB* in the genomic DNA from *M. intracellulare* serotypes 7, 12, and 13 (Fig. 4A). Interestingly, *M. intracellulare* serotype 13 had the same-sized DNA fragment of the *orfA-orfB* region, and the nucleotide sequences were determined. The 1.95-kb *orfA-orfB* regions of the two serotype 13 strains had complete identity and showed only one nucleotide substitution from that of serotype 12: codon 105, TTC, of the *orfB* in serotype 12 was replaced by codon TCC in serotype 13 (Fig. 4B). This missense mutation induced a single amino acid substitution from Phe to Ser and implied the loss of the *orfB* activity for *O*-methylation.

Expression of sero12-*orfB* and sero13-*orfB* in *M. intracellulare* serotype 13. To test the functional activity of *orfB* in *M. intracellulare* serotypes 12 and 13, the sero12-*orfB* and sero13-*orfB* genes were introduced into the *M. intracellulare* serotype 13 strain. The 0.84-kb sero12-*orfB* and sero13-*orfB* were amplified and cloned into a pVV16 vector, and *M. intracellulare* serotype 13 ATCC 35769 was transformed with the resulting plasmids and the pVV16 vector. The alkaline-stable lipids derived from the transformants were developed on TLC plates, and the productive GPLs were compared to the spots of serotype 7, 12, and 13 GPLs (Fig. 5A). Both R_f values of the GPLs produced in the transformants with the pVV16 vector and sero13-*orfB* were identical to that of the serotype 13 GPL. However, the R_f value of the GPL produced in the transformant with sero12-*orfB* was the same as that of serotype 12 GPL. By MALDI-TOF MS, the main molecular weights of the GPLs produced in the transformants with sero12-*orfB*, sero13-*orfB*, and the pVV16 vector were detected as *m/z* 1,911, 1,897, and 1,897, respectively, for $[M+Na]^+$ (data not shown). The fragment ions of the related glycosyl cleavage in the OSEs were analyzed by using MALDI-TOF MS/MS, and the glycosyl compositions were determined. The fragment ions of the OSEs in the pVV16 vector and sero13-*orfB* showed the same pattern as serotype 13 GPL, indicating that overexpression of sero13-*orfB* in the serotype 13 strain was not affected (Fig. 2A and 5B). The fragment ions of the OSE in sero12-*orfB*, i.e., *m/z* 254 and 414, were different from those of the OSE in sero13-*orfB*, i.e., *m/z* 240 and 400, respectively (Fig. 5B). The GC/MS spectrum of the perdeuteromethylated alditol acetate derivative of the terminal *N*-acylated Hex from sero12-*orfB* was assigned to 2-*O*-deuteromethyl-1,5-di-*O*-acetyl-4-2′-*O*-deuteromethyl-propanoyl-deuteromethylamido-4,6-dideoxy-3-*O*-methyl-hexitol from the fragment pattern (*m/z* 62, 105, 121, 165, 206, 222, 266, and 300) (Fig. 5C), which was identical to that of the serotype 12 GPL. These results demonstrated that the serotype 13 transformant with sero12-*orfB* but not sero13-*orfB* had an added *O*-methyl group at the C-3 position in the terminal Hex and that the productive GPL was completely changed from serotype 13 to serotype 12. In addition, we confirmed that the plasmid-deleted C-terminal 40-base region of sero12-*orfB* was completely functional and that sero12-*orfB* worked in the serotype 7 transformant. Taken together, these results indicated that sero13-*orfB* was inactivated by the missense mutation at codon 105 and that the serotype 13 GPL lacked *O*-methylation at the C-3 position of the terminal Hex.

Native conformation of serotype 13 GPL and host response. The native serotype 13 GPL was purified without alkaline treatment. The native serotype 13 GPLs were detected on TLC

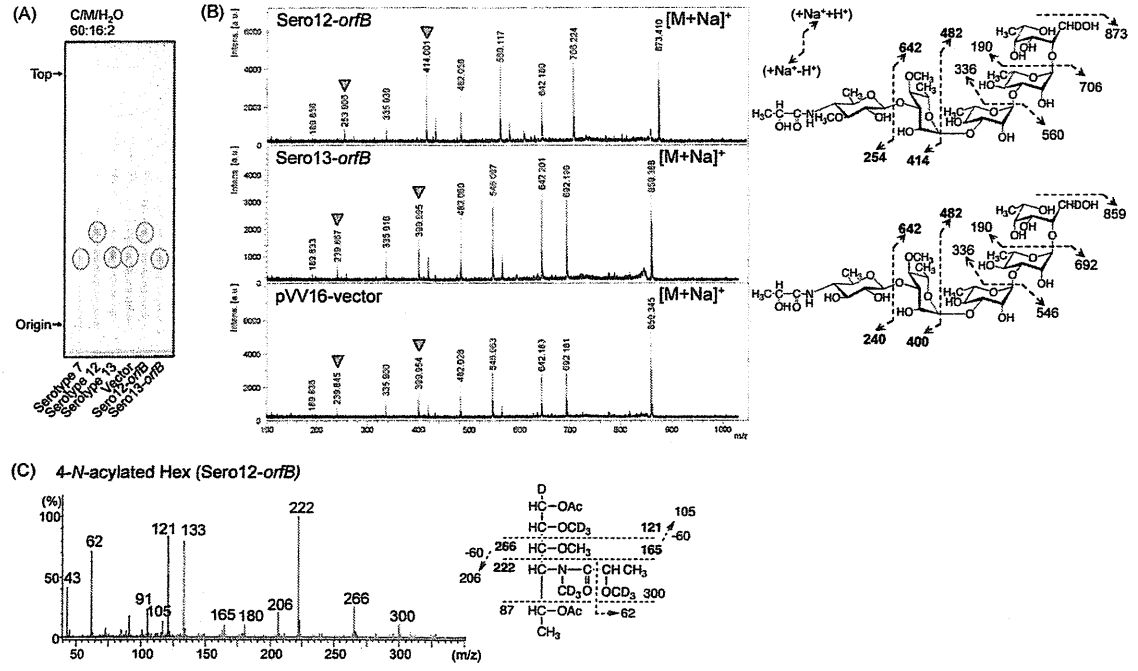

FIG. 5. The productive GPLs in transformants of *M. intracellulare* serotype 13 with sero12-*orfB* or sero13-*orfB*. (A) TLC patterns of the alkaline-stable lipids derived from *M. intracellulare* serotypes 7, 12, and 13 and serotype 13 transformants (ATCC 35769) with the pVV16-vector, sero12-*orfB*, and sero13-*orfB* from left to right, developing with a solvent system of chloroform-methanol-water (60:16:2 [vol/vol/vol]). (B) MALDI-TOF MS/MS spectra of OSEs derived from the productive GPLs in transformants of *M. intracellulare* serotype 13 with sero12-*orfB*, sero13-*orfB*, and the pVV16 vector. The replaced mass numbers are indicated by arrowheads. (C) GC/MS spectrum of the perdeuteromethylated alditol acetate derivative of the terminal *N*-acylated Hex from serotype 13 transformant with sero12-*orfB*. The MALDI TOF MS/MS and GC/MS conditions are described in the legends for Fig. 2 and 3. Ac, CH_3CO.

plates as three major spots that expanded broadly and had R_f values different from that of the alkaline-treated serotype 13 GPL. These spots were converged into one spot by alkaline treatment (Fig. 6A). It was reported that some positions of OSE in GPLs are acetylated in nature (27). The molecular weights of these three spots were checked by MALDI-TOF MS. The mass numbers of *m/z* 1,983, 2,025, and 2,067 for $[M+Na]^+$ caused the 2- to 4-unit increases of *m/z* 42 (addition of acetylations) and the modification to saturated alkyl group, compared to *m/z* 1,897 of the alkaline-treated serotype 13 GPL, implying that native GPLs were modified by several *O*-acetylations in the OSE portion and that alkaline treatment removed the acetylated groups (Fig. 6B). In addition, several peaks at intervals of 14 atomic mass units were caused by an alkyl group, indicating that the fatty acids of the core portion were variable and that the molecular species were heterogeneous.

To clarify the host recognitions of serotype 13 GPL via TLRs, we stimulated HEK-blue-2 and -4 cells with native and alkaline-treated serotype 13 GPLs. The native serotype 13 GPL significantly activated HEK-blue-2 cells in a dose-dependent manner, but HEK-blue-4 cells did not respond. The alkaline-treated serotype 13 GPL without *O*-acetylation did not activate either HEK-blue-2 or -4 cells. Reacetylated alkaline-treated serotype 13 GPLs with *O*-acetyl groups substituted for all hydroxy groups of OSE activated HEK-blue-2 cells, although the level of activation was less than that of the native form (Fig. 6C). Moreover, we confirmed that only the native serotype 13 GPL stimulated mouse bone marrow-derived macrophages via TLR2 by using C57BL/6 and TLR2 knockout mice (see Fig. S2 in the supplemental material).

DISCUSSION

The structural heterogeneity of the GPLs in MAIC species is reflected in their morphology, virulence, and pathogenicity (2, 3, 24) and may be meaningful in phylogenetic classification. Actually, epidemiological studies show that the isolates of MAIC serotypes from patients are heterogeneous and important for assessing the prognosis of pulmonary MAIC disease (25, 37). Chatterjee and Khoo (9) proposed grouping the three types of GPLs by OSE structure, and the group 2 GPLs included the serotype 12, 17, and 19 strains. The serotype 7 and 16 GPLs determined in our previous studies also belong to the group 2 GPLs (13, 14). The group 2 GPLs have in common 6-d-Tal-Rha-Rha and serotype-individual sugars elongated from the second Rha. In addition, except for the serotype 19 GPL, group 2 GPLs carry an unusual substituent, *N*-acylated amido sugar, as the terminal Hex. Aspinall et al. (1) mentioned that the terminal sugar residue of serotype 12 GPL is a derivative of viosamine (4-amino-4,6-dideoxyglucose). The structural difference between serotype 7 and 12 GPLs in group 2 was due to the functions of three methyltransferase genes, *orf2*, *orfA*, and *orfB* (13, 30). In this study, we found that the serotype 13 GPL was structurally very close to those of serotypes 7 and 12, and we determined the novel structure of

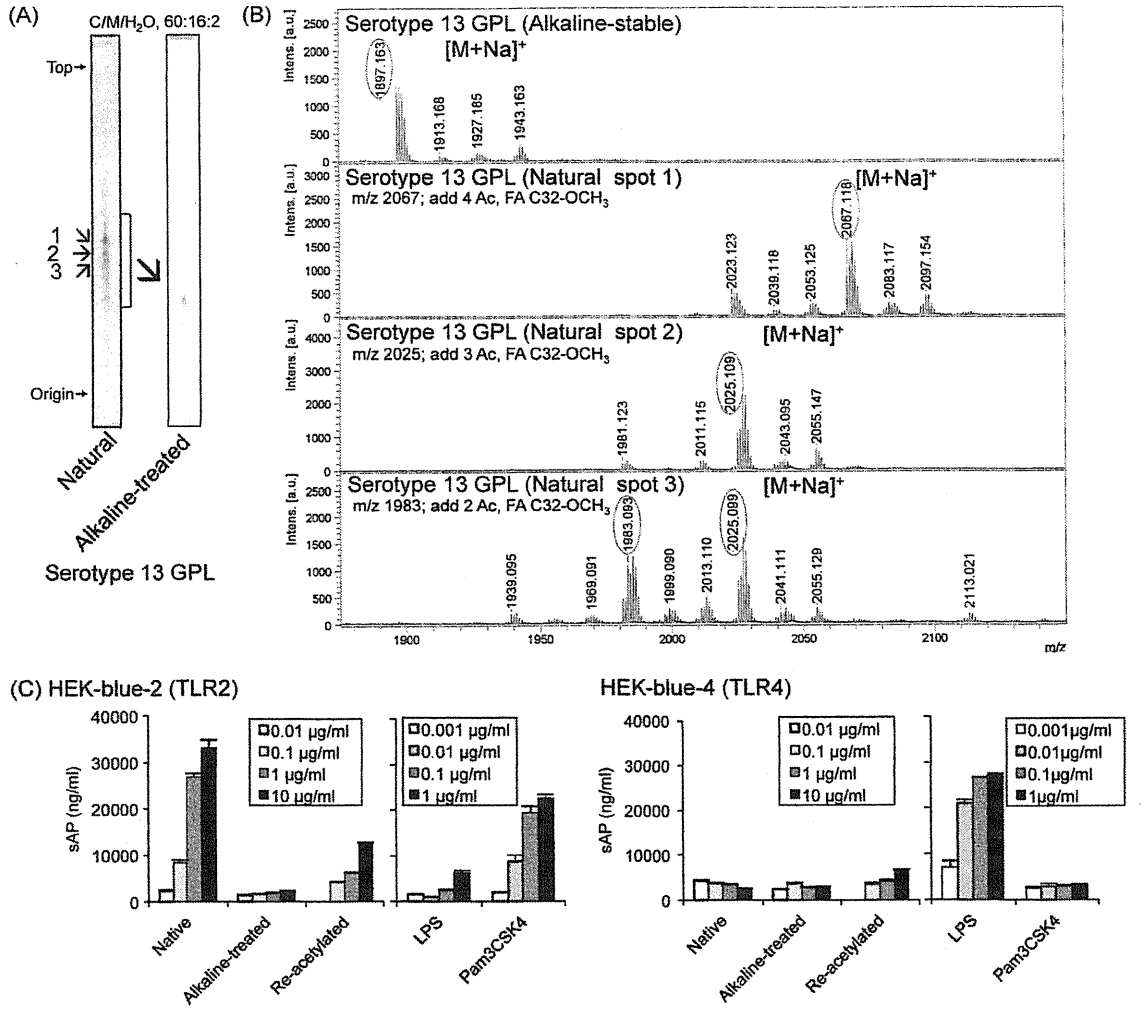

FIG. 6. TLC patterns, MALDI-TOF MS spectra, and TLR recognition of the native and alkaline-treated serotype 13 GPL. (A) The TLC plate was developed with a solvent system of chloroform-methanol-water (60:16:2 [vol/vol/vol]). Three major spots of native GPL are indicated by the numbers from top to bottom. (B) The major spots were purified and their molecular ions were measured by MALDI-TOF MS. The condition is described in the legend for Fig. 1. (C) HEK-blue-2 and -4 cells (2×10^5 cells/ml) were stimulated with native, alkaline-treated, and reacetylated serotype 13 GPLs. After 24 h of incubation, NF-κB activation was assessed by measuring the levels of secreted alkaline phosphatase (sAP) in the supernatant by using QUANTI-Blue. The data are means ± standard deviations (SD) for two experiments done in duplicate.

the serotype 13 GPL to be 4-2′-hydroxypropanoyl-amido-4,6-dideoxy-β-hexose-(1→3)-4-*O*-methyl-α-L-rhamnose-(1→3)-α-L-rhamnose-(1→3)-α-L-rhamnose-(1→2)-α-L-6-deoxy-talose. This result clarified that the serotype 13 GPL is structurally different from the serotype 7 and 12 GPLs in the *O*-methylations of the terminal *N*-acylated Hex and Rha next to the terminal Hex. Serotype 13 GPL lacked the *O*-methyl group in the terminal *N*-acylated Hex, although serotype 7 and 12 GPLs had one at the C-2 and C-3 positions, respectively. The composition and position of the *N*-acyl group at the terminal Hex were completely identical in these three GPLs. At the Rha next to the terminal Hex, serotype 12 and 13 GPLs have an *O*-methyl group at the C-4 position, and this modification is present in all group 2 GPLs except for the serotype 7 GPL, suggesting that this methyl group may play a role in MAIC physiology and virulence. These results also implied that *M. intracellulare* serotypes 7, 12, and 13 are very close phylogenetically.

We investigated the relationship between the structure and biosynthetic pathway and tried to verify the phylogenetic classification of serotypes 7, 12, and 13 by genetic analysis of GPL biosynthesis. We previously reported the nucleotide sequences of the *gtfB-drrC* region, which completely determine each serotype-specific GPL in serotypes 7 and 12 (13, 30), and found the sequence of the serotype 13 gene cluster (unpublished data). The genetic organizations of the *gtfB-drrC* regions in serotype 7, 12, and 13 gene clusters closely resemble each other. Seven common ORFs are conserved in *gtfB-drrC* clusters, suggesting that these three serotypes diverged from a common ancestor. The *orfA-orfB* region in serotypes 12 and 13 replaced *orf2* in serotype 7. Only one nucleotide substitution was found in the 1.95-kb segment in *orfA-orfB* of serotypes 12

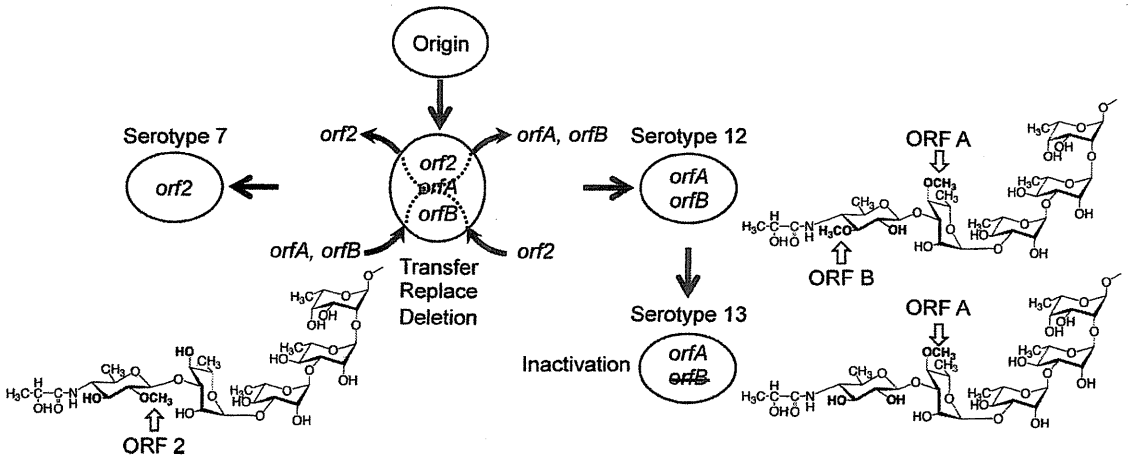

FIG. 7. Scheme of the relationship between GPL biosynthesis ORFs encoded the methyltransferases and their structures.

and 13, and *orfB* in serotype 13 was inactivated. In general, it is unusual for an ORF inactivated by a missense mutation to remain in the genome because it is a burden for the bacterium to transcribe and translate an inactivated ORF. Thus, the *M. intracellulare* serotype 13 strain must have diverged from an *M. intracellulare* serotype 12 organism recently. Serotype 13 GPL also has 4-*O*-Me-Rha. *orfA* is responsible for this methylation. In previous studies, we demonstrated that the *orfB* activity had incapacitated the *orf2* activity, which synthesizes an *O*-methyl group at the C-2 position of the terminal Hex of *M. intracellulare* serotype 7. We also showed that the *orf2* activity was independent of *orfA* activity in *M. intracellulare* serotype 12 (30). The relation of methyltransferases, *orfA*, *orfB*, and *orf2* is summarized in Fig. 7.

GPLs are correlated with colony morphology, sliding motility, biofilm formation, immune modulation, and virulence (2, 3, 16, 34). GPLs have several significant features. They are produced in MAIC species and absent from *Mycobacterium tuberculosis*, making it possible to distinguish MAIC from tuberculous mycobacteria (11, 20). An anti-GPL antibody is produced in the sera of patients and reflects the disease, which is useful in diagnosis and treatment (21, 22, 25). Moreover, it was reported that ethambutol-susceptible and -resistant MAIC strains of serotype 1 had different GPL profiles. The susceptible strain expressed only the polar serotype 1 GPL, and the resistant strain expressed several apolar GPLs. The efficacy of antibiotics may be affected by the GPL profile through differences in cell wall permeability (19). On the other hand, the importance of TLR-mediated responses has been studied in tuberculous infections. Means et al. (28) reported that *M. tuberculosis* activated both TLR2 and TLR4, whereas heat-killed *M. tuberculosis* and *M. avium* activated only TLR2. It was observed that MyD88- and TLR2-deficient mice have increased susceptibility to *M. avium* infection compared to TLR4-deficient and wild-type mice (12). These lines of evidence suggest that TLRs are related to host recognition of the MAIC components containing GPLs and affect MAIC infections. Brennan and Goren (6) first proposed that GPLs were alkaline-stable lipids and made it possible to classify serospecificity by the unique, variable deacetylated OSE sequences (9). We did not detect any biological activity of these alkaline-treated GPLs on splenocytes and bone marrow macrophages of mice in *in vitro* stimulation. Recently, Schorey and colleagues (35, 36) clarified that serotype 1 and 2 GPLs can function as TLR2 agonists and promote macrophage activation in a TLR2- and MyD88-dependent pathway. They reported that the acetylated and methylated groups of GPLs were necessary for GPL-TLR2 interaction as a molecular requirement. In this study, we purified both native and alkaline-treated serotype 13 GPLs and clarified the acetylation patterns of serotype 13 GPL. It was confirmed that the native acetylated form of serotype 13 GPL was recognized via TLR2 and that the deacetylated form by alkaline treatment was not recognized. The serotype 13 GPL has one *O*-methyl group next to the terminal *N*-acylated Hex that was stable regardless of alkaline treatment. Taken together, an acetyl rather than a methyl group was necessary for host immune response via TLR2. The completely acetylated derivative of alkaline-treated serotype 13 GPL partially recovered the HEK-blue-2 activation, compared to the native form containing 2 to 4 acetylated groups. It may be important for GPL-TLR2 interaction to balance the hydrophobicity and hydrophilicity of the molecule. Recht and Kolter (32) reported that the acetylation of GPL affects sliding motility and biofilm formation by deleting the *atf1* gene, which is responsible for acetylation on the 6-d-Tal of GPL core in *Mycobacterium smegmatis*. Rhoades et al. (33) reported that the *Mycobacterium abscessus* GPLs were related to smooth and rough colony morphology and that the GPLs in the outermost portion of the cell wall masked underlying phosphatidyl-*myo*-inositol mannosides involved in stimulating the innate immune response via TLR2. In contrast, our results suggest that the species-specific acetylated GPL is effective in host recognition as a TLR2 agonist independent of phosphatidyl-*myo*-inositol mannosides and that it plays important roles directly in host innate immune responses. Regulating the acetylation of GPL may control the MAIC pathogenicity by, for example, developing the inhibitor of ATF1.

The present study demonstrated the chemical structure and biosynthesis gene cluster of the serotype 13 GPL of *M. intracellulare* and host innate immune response via TLR2. Serotype 13 GPL should be included in group 2 GPLs, and the phylogenetic relationship of serotype 7, 12, and 13 strains was par-